This is a preprint, the final version is subject to change, of the American Mineralogist (MSA)
Cite as Authors (Year) Title. American Mineralogist, in press.
(DOI will not work until issue is live.) DOI: http://dx.doi.org/10.2138/am.2014.4660

Insights into the crystal chemistry of earth materials rendered by electron density distributions: Pauling's rules revisited

G.V. Gibbs*, Nancy.L. Ross*, David.F. Cox‡ and Kevin.M. Rosso+

*Department of Geosciences, ‡Department of Chemical Engineering, Virginia Tech, Blacksburg, Virginia 24061, +Physical Sciences Division, Pacific Northwest National Laboratories, Richland, WA 99352

Only one thing is certain: that nothing is certain. Michael de Montaigne

Abstract

Experimental and calculated electron density distributions determined for oxide and silicate crystals and siloxane molecules provide a new basis for addressing the classic foundation of the crystal chemistry of silicates, including atomic/ionic radii, the radius ratio rule and the nexus between the Pauling bond strength, resonance bond number and bond length. The distributions indicate that the charge density of a bonded oxygen atom is highly distorted with its bonded radius decreasing systematically from ~1.50 Å when bonded to highly electropositive atoms like sodium to ~ 0.65 Å when bonded to highly electronegative atoms like nitrogen. Rather than a single radius, the atom has as many bonded radii as it has bonded interactions. Bonded radii determined for the metal atoms match the Shannon effective ionic radii for the more electropositive atoms, but they depart and increase systematically for the more electronegative atoms. Pauling's first rule is considered to be irrelevant given the asphericity and the range of the bonded radii displayed by the O atom.

A power law regression expression is formulated between the average M-O bond lengths, $\langle R(M\text{-}O)\rangle$, and the average value of the electron density, $\langle\rho(\mathbf{r}_c)\rangle = r\,(1.41/\langle R(M\text{-}O)\rangle)^{4.76}$, at the bond critical point, $\mathbf{r}_c$, between pairs of bonded M-O atoms. The expression applies to a host of crystals and molecules comprising atoms for all rows, r, of the periodic table. The $\langle\rho(\mathbf{r}_c)\rangle$ values correlate

with bond strength and resonance bond strength for the M-O bonded interactions on a one-to-one basis, demonstrating that bond strength is a direct measure of the electron density involved in a bonded interaction and the accumulation of the electron density between the bonded pair. The widespread applications of the Brown-Shannon bond valence model in the Earth sciences and material science owes much of its success to the direct connection that exists between bond strength and the quantum mechanical observable, the electron density distribution. Compelling evidence is presented that supports the argument that the Si-O bonded interactions within siloxane molecules and silicate crystals are fundamentally the same, and that the local Si-O bonded interactions comprising molecules are, at the very core and equivalent to the Si-O bonded interactions observed in silicate crystals. Bond paths between the O atoms comprising shared polyhedral edges are consistent with Pauling's third rule, the shorter the O-O shared edges, the greater the accumulation of the electron density between the O atoms, the greater the stabilization of the shared edges.

Evolution of Atomic Radii

Toward the end of the 19th century, geologists' interests had tapered off from goniometric studies of the outer faces of crystals and their interfacial angles focusing instead on the inner arrangements of the atoms within, with the amateur geologist William Barlow (1883; 1898) speculating that the atoms in a cube of rock salt are not only spherical, but they are arranged in a periodic chessboard pattern in 3D-space. Barlow's insightful conjecture that the atoms are arranged in a periodic three-dimensional pattern was verified thirty years later by the famous X-ray diffraction patterns recorded for zincblende crystals (Friedrich et al., 1912). Sir Lawrence Bragg and his father Sir William .H Bragg were quick to recognize the significance of Barlow's conjecture and the X-ray patterns. Primed with the knowledge that the atoms in crystals are arranged in periodic patterns in 3-space, and that the dimensions of the atoms are comparable with the wavelength of an X-ray beam, the

younger Bragg (1914) built a single crystal diffractometer and recorded a set of diffraction data for a cube of rock salt that confirmed Barlow's brilliant speculations.

But, contrary to Barlow's speculations and Bragg's results, the majority of the chemists and physicists at the time were of the mindset that rock salt is a molecular crystal, composed of discrete diatomic Na-Cl molecules bonded by long-range van der Waals' forces. The famous chemist H. E. Armstrong was so incensed with Bragg's chessboard description of the structure that he wrote, "Professor Bragg asserts that in sodium chloride there appear to be no molecules represented by Na-Cl. The equality in the number of the sodium and chlorine atoms is arrived at by a chessboard pattern of atoms; it is a result of geometry and not a pairing-off of the atoms. This statement is more repugnant to common sense. Chemistry is neither chess nor geometry, whatever the X-ray physics may be." Despite Armstrong's strong rebuke of Bragg's work, the idea that crystals like the alkali halides consist of molecular groups was supplanted shortly thereafter with Bragg's chessboard pattern interpretation of the structures. Indeed, Dalton's idea that all crystals consist of small discrete molecules finally gave way to the realization that the atoms in many crystals are bonded together as giant molecules of visible dimensions rather than ones of microscopic dimensions.

Without a doubt, the determination of the structure of rock salt was a fundamental breakthrough in our understanding of the structures of crystals as periodic arrays of bonded atoms in 3-space, a discovery that not only launched the new field of crystal chemistry but also provided a basis for the framing of Pauling's rules. The structure determination of rock salt set Bragg (1913) junior on a whirlwind determination of a number of crystal structures of minerals , and in a very short time he managed to determine the structures of cubic fluorite (CaF_2), pyrite (FeS_2), cuprite (Cu_2O), sphalerite (ZnS_2), and spinel (Mg_2AlO_4) (Bragg, 1937), together with those for other minerals like diamond (Bragg and Bragg, 1913). In addition to determining the atomic arrangements, attention

was focused on unearthing and understanding the underlying the bonded interactions that govern the formation of the structures themselves (Bragg, 1920). Despite the general belief at the time that many of the minerals that the Braggs studied consist of electrostatically bonded cations and anions, the direction that the younger Bragg took in his studies indicate that he believed the contrary. Indeed, it is apparent that he believed that the forces in minerals are largely atomic in nature, and that the atoms in these materials behave, to a first approximation, as hard largely neutral spheres such that the sum of the radii for a bonded pair of atoms closely matches the interatomic separation between the pair, and that the additive sum of radii applied to a wide variety of materials regardless of the type of bonded interactions.

With his hard sphere atomic consensus and a knowledge of the crystal structures, Bragg (1920) undertook the task of compiling of a set of atomic radii. He made the simple yet reasonable assumption that the radius of the sulfur atom, r(S) = 1.02 Å is equal to one half the S-S bond length, R(S-S) = 2.05 Å, that he had found in his structural determination of pyrite. He next determined the radius of the zinc atom, r(Zn) = 1.33 Å, by subtracting r(S) from the Zn-S bond length, R(Zn-S) = 2.35 Å, that he had determined in his structural analysis of zincblende. The radius for the oxygen atom, r(O) = 0.65 Å, was found by subtracting r(Zn) from the Zn-O bond length R(Zn-O) = 1.97 Å observed in zincite. He concluded that the radii were internally consistent when he found, for example, that $2\times r(Zn) = 2.66$ Å, which matched the average separation, 2.65 Å, that he had observed between the bonded pairs of Zn atoms in crystals of zinc, and that $2\times r(O) = 1.30$ Å, which is comparable with the O-O separation, 1.20 Å, observed in the O_2 molecule. Continuing in this fashion, he generated a set of atomic radii for more than 40 atoms that reproduced the experimental bond lengths typically within 0.06 Å, determined for oxides, sulfides, halides and metals. The success of Bragg's radii in the reproduction of the bond lengths for such a wide variety of materials

indicated, contrary to the ionic lattice energy calculations of Sherman (1932), that the bonded interactions for the materials that he studied have a substantial component of atomic character. It also convinced Bragg and later workers that the atoms in many crystals behave, to a first approximation, as rigid spheres each with a given radius, and that by simply adding the radii of a bonded pair, a reasonable and simple estimate can be made of the length of a bonded interaction.

Nearly half a century after Bragg published his radii, the famous solid state physicist J.C. Slater (1964) used Bragg's consensus that bonded atoms behave as rigid spheres in the compilation of the atomic radii for more than 85 elements and found that the resulting radii reproduce more than 1200 bond lengths for a wide range of crystalline and molecular materials, including oxides, nitrides, sulfides, halides, intermetallic compounds and metals, to within 0.12 Å, on average. He also found that the atomic radii correlated with the radii of the outermost valence shell of electrons for the atoms as calculated by relativistic self-consistent field quantum mechanical methods. Slater considered his radii together with Bragg's to be global in their application in that they reproduce bond lengths for all materials reasonably well, particularly considering that the radii, unlike the ones determined later, were not modified to correct for such factors as coordination number, electronic spin, oxidation state, covalency, repulsive forces and polyhedral distortion.

Evolution of ionic radii

In 1926, the Bragg School (Bragg, 1937) undertook the heroic task of solving the crystal structures of the rock-forming silicates. Among other things, Bragg found that the O atoms of forsterite, Mg_2SiO_4, are arranged in a hexagonal close-packed pattern with the Si and Mg atoms tucked away, respectively, in the available tetrahedral and the octahedral voids of the array. On the basis of this observation it was concluded that the oxygen atoms are actually in contact and closest-packed, and that they are substantially larger in size than the Si and Mg atoms. With this finding, he concluded

that the diameter of the O atom must equal half of the average O-O distance, between the adjacent O atoms, 2.70 Å, resulting in a radius of 1.35 Å, a value notably different from his previously determined atomic radius of 0.65 Å. Given his incredible objectivity, Bragg rejected his own atomic radii out of hand in favor of an ionic model with large oxide O^{2-} anions and relatively small $Si^{4+}$and Mg^{2+} cations, despite the fact that his earlier determined atomic radii reproduce bond lengths typically within 0.06 Å of their experimentally measured values.

Bragg's atomic radii were revised shortly after they were published to conform with the popular ionic model proposed by Wasasjerna (1923), who partitioned experimentally determined bond distances into cationic and anionic parts, based on the molar ionic refractivities of the bonded cations and anions. On the basis of this partitioning, a set of ionic radii was determined that resulted in a radius of 1.32 Å for the oxide anion, which was generally accepted as satisfactory given that it agreed with the average separations between the O atoms observed in a number of oxides, including forsterite. The famous geochemist V.M. Goldschmidt (1954) followed Bragg's strategy where it was assumed that bonded cations and anions behave as rigid spheres, each with a unique radius. By systematically subtracting the radius of the oxide anion (1.32 Å) from the M-O bond lengths determined for a number of oxides, a popular set of ionic radii for oxides, sulfides and selenides was ultimately determined that bore Goldschmidt's name, radii that were used well into the 1960s. Recognizing that anions are substantially more polarizable than cations (Fajans, 1931), Goldschmidt (1954) expressed concern about the extent to which the polarizing power of the bonded cations might impact on the radius of the oxide anion, but because at the time little was known as to how to correct ionic radii for the effects of polarization, he had little or no choice but to discount the effect. As his radii were found to be additive and to reproduce the bond lengths for a wide range of

materials, it was assumed that polarization must have some sort of compensating effect that did not impact the bond lengths.

In addition to determining ionic radii and evaluating the impact of cation substitution on the crystal chemistry of minerals, the Goldschmidt School focused its attention on determining the principles that govern the crystal structures of simpler materials, crystal form, isomorphism and polymorphism, in terms of the ionic model; they were also interested in determining what factors govern the coordination numbers of cations. The Bragg School had similar and complementary aspirations, but with the goal of determining and understanding the more complicated structures adopted by the rock forming silicates such as forsterite, diopside ($CaMgSi_2O_6$) (Warren and Bragg, 1928), and tremolite ($Ca_2Mg_5(Si_4O_{11})_2(OH)_2$) (Warren, 1929). Based on the relative sizes of the ions and the structural details, the structures determined for both diopside, and tremolite were described as close-packed structures built from polyhedra with the smaller Si cations coordinated by four oxide anions disposed at the corners of tetrahedra and comprising chains of indefinite extent, with the larger Mg cations coordinated between the chains of tetrahedra by six anions at the corners of octahedra. The even larger Ca cations were found to be coordinated by eight anions disposed at the corners of larger and more irregular polyhedra at the edges of the chains. The H cation in tremolite was assumed to be bonded to an oxide anion, forming an OH anion, which was incorporated as part of the large close-packed assembly of anions. The anions were considered to be so large that their packing, together with the incorporated cations, was thought to govern the structures adopted by the silicates (Bragg, 1937). Goldschmidt and his colleagues were quick to grasp the importance of describing a crystal structure in terms of close-packed large anions disposed in coordination polyhedra, with the smaller cations residing in the voids between the polyhedra and constrained by the local charge balance provided by the anions. On the basis of the ionic radii, the Goldschmidt School concluded that the

coordination numbers adopted by the cations are determined in large part by radius ratio considerations of the bonded cations and closest-packed anions, as proposed earlier by Hüttig (1920), who observed that the smaller the ratio, the smaller the expected coordination number of the cation. It was within this context that Goldschmidt showed that his radii serve to predict bond lengths and cation substitutions, thus providing a basis for understanding isomorphism, and that the radius ratio of a cation and anion could be used to predict the coordination numbers adopted by the cation. It was with these ideas and concepts that Pauling (1929) formulated his first rule that defined the nexus between the ionic radii, the bond lengths, the radius ratio and the properties of the coordination polyhedra of anions housing the cations required for the creation of a stable crystal:

'A coordinated polyhedron of anions is formed about each cation, the cation-anion distance being determined by the radius sum and the coordination number of the cation by the radius ratio.'

Since the advent of this rule, a variety of evermore comprehensive and precise sets of ionic radii were determined based on various atomic properties, for example, the effective nuclear charge and the implications of the Born-Landé equation (Pauling, 1927), the ionization potential (Ahrens, 1952), experimental isothermal compressibility, thermal expansion data and cohesive energies for the bonded atoms (Tosi, 1964; Tosi and Fumi, 1964). For a comprehensive review of the strategies followed by workers in determining ionic radii, see the excellent account by Shannon and Prewitt (S&P) (1969).

As of today, the most precise and comprehensive sets of effective ionic and crystal radii for oxide crystals were compiled by S&P and later revised by Shannon (1976), using more than a 1000 experimentally determined accurate M-O bond lengths. In deriving the radii, a preliminary estimate of the effective ionic radius for each cation was first obtained by subtracting an assumed radius (1.40 Å) for the oxide anion from the experimental M-O distance which, in turn, was then corrected for the

coordination numbers of both the oxide anion and the bonded cations and other factors that were deemed to impact the bonded interactions. A similar strategy was employed in the derivation of a second set of tailor-made radii referred to as crystal radii, derived by assuming a smaller radius for the anion, 1.24 Å. The second set of radii was derived because the assumption of the larger 1.40 Å radius for the anion resulted in unrealistic negative effective ionic radii for several of the more electronegative cations. By dint of the negative radii, workers were urged to use crystal radii when considering the properties of crystals with close-packed anions, and modeling processes such as cation diffusion in minerals and melts (Zhang and Cherniak, 2010). Despite this caveat, both sets of radii have been used with considerable success to date as they reproduce within 0.01Å the average experimental bond lengths for a wide variety of coordinated oxide polyhedra within crystals and molecules. In addition to the unsatisfactory negative effective ionic radii encountered by S&P (1969), there were a number of cases in which there was disagreement between the experimentally determined coordination numbers adopted by the cations in crystals and those predicted from radius ratio considerations. On the other hand, when the crystal radii were employed the agreement with experimentally determined coordination numbers was more satisfactory, supporting their preferred use.

Despite the negative radii and the radius ratio discrepancies, both sets of radii have found widespread use in almost all branches of science, having been cited more than an astounding 30,000 times and have thus advanced our understanding and modeling of material properties. In addition to reproducing bond lengths to within ~ 0.01 Å of the experimental values, the radii have proven to be of considerable use in advancing the understanding of crystal chemistry when used, for example, in the construction of 'stability field' diagrams that delineate the relative stability of a structure in terms of the radii of the substituent atoms, as done, for example, for the spinels, the olivines, the phencites

and related structures (Muller and Roy, 1974) and the silicate garnets (Novak and Gibbs, 1971). They have also found substantial use in the modeling of the conductivity of ions, defects, site preferences, ion diffusion in minerals and melts, chemical zoning, size discrimination and leaching, and modeling of trace elements and distribution coefficients among coexisting phases.

In a study of bond type, Fyfe (1954), asserted that too much emphasis has been placed on the actual radii of atoms in terms of their capabilities to reproduce bond lengths. He posited that the radius of an atom is unlikely to be fixed; particularly when one is mindful that radii of atoms in ionic, atomic, metallic and van der Waals materials are typically assigned different values. In addition, prior to Shannon's (1976) publication of his revised radii, Johnson (1973) reported that the radii of anions like O and S atoms are not fixed, but that they are highly dependent on the polarizing power of the bonded M atoms, with the radii of both ions decreasing systematically with decreasing bond length as the polarizing power of the bonded atoms increase. On the contrary, Pyykko (2012 and references therein) recently compiled a precise set of covalent radii for a variety single-, double- and triple-bonded M-S interactions within a large number of sulfide molecules, and reported little or no evidence that the radius of the S atom is impacted by the bonded interactions. Not only do the covalent radii reproduce the bond lengths for molecules, but they also reproduce to within 0.01 Å the bond lengths observed for binary crystals like ZnS, ternary crystals like $CuInS_2$ and quaternary crystals like Cu_2ZnSnS_4 (see also Cahen, 1988). But, Pyykko's radius for the S atom (1.04 Å) is smaller than the crystal radius (1.70 Å) assumed by Shannon (1981) in the derivation of his crystal radii for sulfide crystals. With these two different sets of radii, one covalent and the other crystal, it is clear that the two different, yet consistent, sets of radii for sulfides can be generated by assuming two different radii for the S atom, both capable of reproducing sulfide bond lengths, bearing out

231 Fyfe's contention that too much stock has been placed on the actual values assumed for the radii of
232 atoms.

233
234 **Introduction to bonded radii and evaluation of Pauling first rule**

235 In an examination of whether the electron density distribution (ED) of the O atom is largely
236 unaffected by its bonded interactions, such that it retains the distribution of an isolated atom with a
237 fixed radius (Bohórquez and Boyd, 2009) or whether, as reported by Johnson (1973), it is distorted
238 to some degree by the bonded interactions, Gibbs et al., (2013a) undertook a determination of the
239 bonded radii of the atoms comprising a relatively large number silicates and oxides. The goal was to
240 assess the extent to which the ED distribution of a bonded O atom departs, if at all, from the
241 distribution of an isolated atom. It was also of interest to learn how the radii of the metal atoms,
242 estimated from the ED distributions, correspond with the S&P radii, and how they vary with the
243 coordination number and the row number of the atoms. We note that we follow Pauling (1960,
244 section 2-9) and other quantum chemists and consider Li, Be, B..., as first row atoms and Na, Mg,
245 Al,... , as second row atoms and so on.

246 It is mindful that the ED distribution of a material is not only a quantum mechanical observable, but
247 that it is a robust property that contains all the information that that can be measured for a material,
248 including its potential, kinetic and total energies (Parr and Yang, 1989). In a stable crystal free of
249 defects, the distribution, together with the nuclei of the atoms, are distributed in a periodic pattern in
250 3-space such that the total energy of the resulting configuration of the bonded atoms is minimized
251 and the force on each atom is zero (Feynman, 1939).

252 The efforts of the renowned quantum chemist Professor Richard F. W. Bader (1990) and his
253 coworkers has resulted in a basis, founded on the ED distributions, for determining whether or not a

pair of atoms is bonded. A pair is considered to be bonded only if there exists a continuous pathway of maximum ED (denoted as the bond path) that connects the nuclei of the pair (Bader, 2009). Along the path there exist one, and only one, point where the ED distribution adopts a local minimum value, denoted as the bond critical point, $\mathbf{r}_c$, of the bonded interaction. As the position of the point is well-defined, the accumulation of the ED at $\mathbf{r}_c$ is taken as a unique measure of the strength of a bonded interaction: typically, the greater the accumulation and the concentration of ED at $\mathbf{r}_c$, the shorter the bonded interaction. Furthermore, as the bonded atoms in a structure are connected by bond paths, the total number of bond paths that radiate from a given atom to the other atoms to which it is bonded serves to define uniquely the coordination number of the atom.

As asserted by the Nobel prize winning chemical physicist Robert Mulliken, 'the concept of 'the chemical bond is not so simple as some people think.' Indeed, as a chemical bond is not even a quantum mechanical observable, given that there is no known non-arbitrary linear Hermitian operator that contains a complete set of eigenfunctions that can be associated with a chemical bond, Bader (2009) pointed out that a chemical bond cannot be identified by either a bond path or a bonded interaction. More than half a century ago, the famous mathematician-chemist Charles A. Coulson (1955) asserted that "A chemical bond is not a real thing: it does not exist, no one has ever seen it, no one ever can. It is a figment of our imagination." Well aware of this assertion, Bader pointed out that 'There are no bonds between pairs of atoms, only bonded interactions' (2009). Hoffmann (1988) went on to say 'Physicists do not see bonds, they only see bands.' Given these inconvenient truths, Cremer and Kraka (1984) reiterated that 'There is no way to measure a bond or a bond property.' They continued by asserting that a bonded interaction can only be defined within the framework of a model like Bader's topological model of the ED distribution, which provides a unique basis for

defining a bonded interaction, bond strength and the bonded radii for atoms in molecules and crystals.

As the bond critical point between a pair of bonded atoms is uniquely defined, the properties of the ED at $\mathbf{r}_c$ have been used by a large number of workers to characterize bonded atom pairs (cf. Gatti, 2005). The bonded radii for a bonded pair of M and O atoms, denoted $r_b(M)$ and $r_b(O)$, are defined as the distances between the nuclei of the pair and $\mathbf{r}_c$, respectively (Bader, 1990). As observed above, the accumulation of the ED at $\mathbf{r}_c$, $\rho(\mathbf{r}_c)$, is taken as a measure of the relative strength of a bonded interaction, as observed above, typically the larger the value of $\rho(\mathbf{r}_c)$ the stronger the bonded interaction and shorter bond length. The negative curvatures of the ED at $\mathbf{r}_c$ along two mutually perpendicular directions that lay perpendicular to the bond path, denoted as λ_1 and λ_2, measure the extent to which $\rho(\mathbf{r})$ is locally concentrated at $\mathbf{r}_c$, perpendicular to the bond path. The positive curvature of $\rho(\mathbf{r})$ parallel to the bond path at $\mathbf{r}_c$, denoted λ_3, serves as a measure of the extent to which the ED is locally concentrated parallel to the bond path at $\mathbf{r}_c$ in the directions of the bonded atoms, in effect, serving to shield the nuclei of the bonded pair. The Laplacian of $\rho(\mathbf{r})$ at $\mathbf{r}_c$, denoted $\nabla^2\rho(\mathbf{r}_c)$, not only serves to measure the extent to which the ED is locally concentrated at $\mathbf{r}_c$, but it has also been used to assess the character of a bonded interaction in an assessment of whether it is shared a covalent, polar covalent, or closed shell ionic bonded interactions (Bader and Essen, 1984; Bader, 1990).

The bond critical point (bcp) properties for the Si-O bonded interactions, calculated for more than 50 silicate crystals and siloxane molecules, are displayed in Figure 1 in terms of their experimental Si-O bond lengths, R(Si-O) (Gibbs et al., 2001). In the calculations, the Gaussian basis wave functions and the energies for the crystals were calculated within the density functional theory framework with the software *CRYSTAL98* (Saunders et al., 1998). The local energy density

properties together with the other bcp properties for the bonded interactions were calculated with *TOPOND* (Gatti, 1997). The geometry optimized structures for the molecules were calculated with *Gaussian 90*, and the bcp properties were calculated with software *EXTREME*, which was kindly supplied by Professor Bader. As evinced by Figure 1a, as $\rho(\mathbf{r_c})$ increases in value, the experimental Si-O bond lengths decrease systematically, with the shorter bond lengths tending to involve larger values of $\rho(\mathbf{r_c})$. The two negative curvatures, λ_1 and λ_2, of $\rho(\mathbf{r}_c)$ for the bonded interactions were averaged and the averaged magnitudes for the pair, $\lambda_{1,2} = ½ |(\lambda_{1+} \lambda_2)|$, are plotted in Figure 2b in terms of R(Si-O). As $\lambda_{1,2}$ increases, R(Si-O) decreases in tandem, demonstrating that $\rho(\mathbf{r})$ is progressively concentrated in the internuclear region as a result of the progressive contractions of the ED toward the bond path (Bader, 1990). For all of the Si-O bonded interactions used to prepare Figure 1, λ_1 and λ_2 are virtually identical in value, an observation that shows that the ED distributions perpendicular to the bond path at $\mathbf{r}_c$ of the Si-O bonded interactions are largely circular in cross section, as observed for diatomic molecules. As noted above, the curvature of the ED at $\mathbf{r}_c$, determined parallel to the bond path (denoted λ_3), measures the extent to which the ED is locally concentrated toward the Si and O atoms, with an increase in λ_3, resulting in a greater shielding of the Si and O atoms with decreasing bond length. As indicated by Figures 1b and 1c, the contraction of ED away from the bcp along the Si-O bond path is greater than the contraction perpendicular to the bond path. As $\nabla^2\rho(\mathbf{r_c}) = \lambda_1 + \lambda_2 + \lambda_3$ (Bader, 1990) and as $\lambda_3 > 2\lambda_{1,2}$, $\nabla^2\rho(\mathbf{r_c})$ is necessarily positive. The magnitude of $\nabla^2\rho(\mathbf{r_c})$ indicates that the shared polar covalent character of the Si-O bond increases as the Si-O bond length decreases for reasons associated with the connection between the Laplacian and the local kinetic and potential energies of the Si-O bonded interactions, as discussed elsewhere (Gibbs et al., 2012).

The bcp properties determined experimentally for the Si-O bonded interactions for the two silica polymorphs, coesite (Gibbs et al., 2003) and stishovite (Kirfel et al., 2001), are added to Figure 1 for sake of comparison with values calculated for the silicate crystals and siloxane molecules (Gibbs et al., 2004). The agreement between the two is generally good, with the experimental values following the general trend of calculated data, demonstrating that the precision of the calculated bcp properties is comparable with experimental properties determined for both coesite and stishovite. This bodes well for the future employment of calculated bcp properties for modeling the properties and bonded interactions of crystals and giving a faithful representation of the properties.

Figure 1e shows that the calculated and experimental bonded radii for the O atoms, r_b(O), bonded to Si atoms are not fixed, but that they decreases linearly from ~ 1.1 Å to ~ 0.9 Å as R(Si-O) decreases by a comparable amount from ~1.8 Å to ~1.6 Å. This result demonstrates the impact that the polarizing power of the bonded Si atoms has on the radius and charge distribution of the O atom, similar to a finding made by Johnson (1973). His study revealed that the radius of the O atom is not fixed but decreases systematically from ~1.40 Å when bonded to K (with an effective polarizing power of 0.87) to ~1.0 Å when bonded to Be (with an effective polarizing power of 1.44). Shannon and Prewitt (1969) anticipated the potential polarizing impact of the bonded cations on the ED distribution and radius of the oxide anion, but had no satisfactory way of reckoning with the problem. But, as their radii are additive and to reproduce the bond lengths for a wide range of materials, it is likely that they assumed, as done earlier by Goldschmidt, that the impact of the polarization must have had some sort of compensating effect that had little or no affect on the bond lengths.

The distribution of the individual bonded radii for the O atom and the associated experimental bond lengths for the M-O bonded interactions, comprising the silicates and oxide crystals, is displayed in

Figure 2 (Gibbs et al., 2001). Consistent with the linear trend displayed in Figure 1e, well-developed trends are observed between the bond lengths and the bonded radii of the O atom, with r_b(O) decreasing linearly along parallel trends for the bulk of the bonded interaction with decreasing bond length, R(M-O.) In contradiction with the assumption that the radius of the oxide anion is largely fixed, r_b(O) displays a wide range of values from ~1.50 Å when bonded to the electropositive Na atom to 0.65 Å when bonded to the electronegative N atom. The smaller value is identical with Bragg's (1920) atomic radius for the O atom, while the larger is comparable to Pauling's (1927) ionic radius of 1.40 Å. It is also evident that the greater the electronegativity of a bonded M atom (for a given row of the periodic table), the shorter the M-O bond length and the smaller the bonded radius of the O atom. The bonded radius of the O atom associated with the Be-O bonded interactions, for example, ranges between 1.01 and 1.10 Å with an average value of 1.07 Å, in agreement with the value of 1.0 Å reported by Johnson (1973). In the case of the Mg-O bonded interactions, the value of r_b(O) displays an even wider range of values, and changes from1.07 Å to 1.31 Å as R(Mg-O) increases from 1.91 Å to 2.27 Å, with an average radius of 1.2 Å, a value that again is in agreement with the value found by Johnson (1973).

The average radii for the O atoms, $\langle r_b(O) \rangle$, together with the average bonded radii for the first, second and third row metal atoms, $\langle r_b(M) \rangle$, determined for a large number of different M-O bonded interactions, including silicate and oxide crystals and molecules, are given in Table 1, along with the corresponding Shannon (1976) crystal, r_c(M) and effective ionic, r_i(M), radii for the bonded M cations. The systematic increase of R(Mg-O) with increasing r_b(O) (Table 1, Figure 2) is ascribed to a systematic increase in *both* r_b(Mg) and r_b(O), with R(Mg-O) increasing systematically with increasing coordination number for the Mg atom as $\langle r_b(O) \rangle$ increases likewise. Surprisingly, the increase in the bonded radius of the O atom is almost twice that of the increase in the Mg radius as

367 the coordination number of Mg increases from 4 to 8. In effect, the increase in R(Mg-O) is due more
368 to the increase in $<r_b(O)>$ than to the increase in $<r_b(Mg)>$, contrary to the assumption that the
369 increase in coordination number results only in the increase of the Mg atom radius. The bonded radii
370 in Table 1 show that the increase in the M-O bond lengths with increasing coordination number for
371 the M atoms is generally due to a greater increase in $<r_b(O)>$ than $<r_b(M)>$. Rather than being
372 dependent entirely on the increase $r_b(M)$ with increasing coordination number, the increase in the
373 bond lengths (Figure 2) can be ascribed to a combined increase of both $<r_b(O)>$ and $<r_b(M)>$, with
374 the bulk of the increase due to the increase in $<r_b(O)>$.

375 Associated with the progressive increase in $<r_b(O)>$ with increasing bond length, the bonded radii
376 for the M atoms (Table 1) are typically larger than the S&P effective ionic radii, $r_i(M)$, particularly
377 for the more electronegative M atoms (Table 1). It is clear that if a smaller radius had been assumed
378 for the oxide anion, negative cation radii (e.g. H, ^{III}C and ^{III}N) would never have been realized. For
379 example, when S&P assumed a radius of 1.24 Å for the oxide anion, only the hydrogen cation has
380 negative crystal radius.

381 The averaged bonded radii for the metal atoms, $<r_b(M)>$, are plotted in Figure 3 in terms of their
382 averaged bond lengths, <R(M-O)>. As the bond lengths decrease, the radii for row 1, 2 and 3 M
383 atoms scatter along three distinct and roughly parallel trends, a feature that is most apparent for the
384 row 2 and 3 atoms (Gibbs et al., 2013a). The trends are also comparable with that found when the
385 radii of the maximum radial charge density distributions of the outermost shells for the M atoms and
386 Slater's empirical radii are plotted relative to the atomic number of the atoms (Slater, 1965). These
387 trends in rows are consistent with <R(M-O)> and $\rho(\mathbf{r}_c)$ trends reported for silicate and oxide crystals
388 (Gibbs et al., 2013a).

Unlike the bulk of the metal atoms, the bonded radius of first row ^{III}N atom actually increases with decreasing bond length. The radius of the ^{III}C atom also departs from the first row trend but, unlike ^{III}N, its radius is much less dependent on the bond length. These observations are ascribed to the relatively large contraction of ED distribution of the O atom by the highly polarizing impact of ^{III}C and particularly ^{III}N. The end result is a substantial contraction of the ED distribution of the O atom along the N-O bond path, an increase in the value of $\rho(\mathbf{r}_c)$, together with a displacement of the bcp toward the O atom, a substantial increase in the bonded radius of the N atom, and a decrease in the bonded radius of the O atom. In effect, the displacement results in a decrease in bonded radius of the O atom with a concomitant increase in the bonded radius of ^{III}N. The ^{III}C-O bonded interaction displays a hint of the same trend with the r_b(C) and C-O bond length, with the radius of the electronegative C atom tending to follow the same trend displayed by the ^{III}N atom. Given that the O atom is much more polarizable that than the nitrogen atom (Johnson et al., 1983; Shannon and Fischer, 2006), the substantial increase in the bonded radius of the N atom and the substantial decrease in the radius of the O atom may be expected.

As the electronegativities of the M atoms bonded to the O atoms decrease and the M-O bond lengths increase, the average bonded radius of the O increases systematically: 0.65 Å when bonded to ^{III}N, 0.83 Å when bonded to ^{III}C, 0.89 Å when bonded to ^{IV}S, 0.95 Å when bonded to ^{IV}Si, 1.00 Å when bonded to ^{IV}Al, 1.20 Å when bonded to ^{VI}Mg, 1.35 Å when bonded to ^{VI}Na, and 1.43 Å when bonded to ^{VI}K. It is apparent that the highly electropositive potassium atom has little or no impact on the ED distribution of the O atom as its bonded radius closely matches Pauling's 'unpolarized radius' for the oxide anion, 1.40 Å.

Concomitant with the decrease in $\langle r_b(O) \rangle$ and M-O bond length with increasing electronegativity of the bonded M atom, the effective ionic radii, r_i(M), of the M cations decrease in tandem with

412 $<r_b(M)>$, but at a faster rate as the bond lengths decrease, resulting in unrealistic negative effective
413 ionic radii for ^{III}C, ^{III}N and H. The crystal radii also decrease with decreasing bond length, but as
414 they were derived assuming a small radius for the oxide anion, only the H cation has a negative
415 crystal radius. Unlike the ionic and crystal radii, the bonded radii for the metal atoms necessarily
416 remain positive, and become progressively larger than the ionic radii with decreasing bond length,
417 with the bonded radii exceeding the ionic radii by as much 0.70 Å in the case of the nitrogen atom.

418 Given the assorted field strengths of the metal atoms and the different M-O bond lengths, the ED of
419 the O atom is rarely, if ever, spherical as traditionally assumed, but as observed above, it often
420 displays several different radii when bonded to different M atoms. Such differences in the radius of
421 the O atom are particularly noticeable when it is bonded to metal atoms with substantially different
422 electronegativities (O'Keeffe and Hyde, 1981). As a case in point, the O_{Al} oxygen atom of the
423 tetrahedral framework of the alkali feldspar maximum microcline, $KAlSi_3O_8$, is bonded to a ^{IV}Si
424 atom (Si-O bond length = 1.61 Å), an ^{IV}Al atom (Al-O bond length = 1.76 Å), and two ^{VI}K atoms
425 (average K-O bond lengths = 2.85 Å). The bonded radius of the O atom along the bond vectors for
426 these four bonded interactions decreases systematically from 1.43 Å along each of the two K-O bond
427 vectors, to 1.01 Å along the Al-O bond vector, to 0.95 Å along the Si-O bond vector. As expected,
428 the electronegativities for the three atoms increase from 2.42 eV for K, to 3.23 eV for Al, and to 4.77
429 eV for Si (Table F.1, Parr and Yang, 1989) as the associated bond lengths and bonded radii decrease.
430 With the different electronegativities and bond lengths of the bonded interactions, the resulting ED
431 distribution of the O atom is highly aspherical with its dimensions being undefined in all other
432 directions, except along the ^{VI}K-O, ^{IV}Al-O and ^{IV}Si-O bond vectors. Given the relatively large range
433 in the bonded radii and the asphericity of the ED distribution of the O atom, it is questionable
434 whether the word 'radius' has meaning in this context, as pointed out by O'Keeffe and Hyde (1981).

435 Not only is the radius undefined in this context, but the radius of O_{A1} and the radius ratio of the
436 bonded atoms are undefined as well, primarily because of the different bonded radii observed along
437 the bond vectors of the bonded atoms.

438 As observed above, the coordination number of an atom can be found, regardless of whether or not
439 the radii of the atoms are known, simply by counting the number of bond paths that radiate from the
440 atom. In the case of microcline, there are nine nearest neighbor O atoms that encroach upon the K
441 atom at distances ranging from 2.75 Å to 3.13 Å (Downs et al., 1996). Given that the effective ionic
442 radii for K^+ and O^{2-} are practically the same, one may conclude from radius ratio considerations that
443 the coordination number of the K cation is either eight or possibly twelve. But an evaluation of the
444 bcp properties for the feldspar shows that there are only six bond paths that radiate from the K atom
445 to six of the nearest O atoms. Accordingly, on the basis of the ED distribution, the coordination
446 number of the potassium is six, much smaller than twelve as specified by the radius ratio.

447 Given the asphericity and the range in the bonded radii displayed by the O_{A1} atom, one questions
448 'Whether Pauling's first rule is useful and applicable or whether it should it be completely
449 abandoned with no alternative?' Coupled with the observation that the bonded radius of the O atom
450 highly is dependent on its bonded interactions, we believe that these contradictions are sufficient to
451 abandon the rule.

452 With these contradictions, we question 'Why have crystal and effective ionic radii been so successful
453 in modeling such properties as chemical zoning, ion conductivity, defects, size discrimination,
454 among other things, predicting coordination numbers when the bonded radius of the O atom varies
455 substantially from 0.64 Å when bonded to ^{III}N and 1.43 Å when bonded to ^{VI}K, values that depart
456 substantially from the values of $r_i(O)$ and $r_c(O)$?' The main reason for the successful use of the radii
457 is that they are highly correlated, on a one to one basis, with the average experimental M-O bond

lengths used in their determination so that any property that correlates with and depends on the cation radius will necessarily correlate with and depend on the bond length involving the cation and *vice versa.* After all, it is the bond lengths that were determined experimentally and that depend on the energetics of the bonded interaction, not the ionic radii (Gibbs et al., 2008b). It is important to note that no matter what choice is made for the radius of the O atom (within reason) used in the determination of a set of radii from a set of average experimental bond lengths, a set of metal radii will necessarily result which when added to that of the O atom will necessarily reproduce the bond lengths. As a case in point, S&P assumed a radius of 1.40 Å for the oxide anion in the derivation of their ionic radii and a radius of 1.24 Å in the derivation of their crystal radii. As expected, despite the assumption of different radii for the oxide anion, the resulting sets of radii resulted in sets of calculated bond lengths that match the experimental bond lengths to within 0.01 Å, on average.

Pauling's second rule

Pauling's second rule was obtained in part from a comprehensive knowledge of the crystal structures of minerals and other materials known prior 1929, from Born's early work on crystal energy, and likely from Pauling's knowledge of resonance theory for the bonded interactions in molecules. It is important to realize that the rule was considered to be neither rigorous nor global in its application, but as pointed out by Pauling (1939), it has been successfully used to verify crystal structures. As asserted by Bragg (1937), the rule seems to be manifest in the condition of a system of low potential energy and, accordingly, high stability. He also observed that although the rule appears to be simple, it imposes rigorous constraints on the topology of the bonded interactions within a structure. Pauling (1960) was well aware that his rules may well have significance for molecules, for which he associated the bonded interactions with resonating bond numbers as representing the strengths of the bonded interactions. As minerals and related materials were considered by many at the time to

consist of spherical ions bonded together by long range electrostatic isotropic bonded interactions, he defined the strength of each bonded interaction to be $s = z/\nu$ where z is the number of electrons involved in the bonded interaction, ze is the electrical charge of the cation, and ν its coordination number. With these definitions, he postulated that:

In a stable ionic structure the valence of each anion, with changed sign, is exactly or nearly equal to the sum of the strengths of the electrostatic bonds reaching it from adjacent cations where $-\zeta e$ *is the electric charge of the anion and the summation is taken over the cations at the centers of all the polyhedra of which the anion forms a corner; that is*

$$\zeta = \sum_i s_i = \sum_i \frac{z_i}{\nu_i}$$

the summation being taken over the bonded cations at the centers of all the polyhedra of which the anion forms a corner.

Despite its simplicity, the rule has been used extensively in the rationalization of the bonded interactions in crystals in terms of the nexus between the bond strength and bond length. Furthermore, the definition of bond strength closely resembles Pauling's definition of resonance bond number used to rank the resonating C-C bonded interactions in molecules and crystals; the larger the resonating bond number the greater the strength and the shorter the C-C bonded interaction (Pauling, 1960). In a related study, resonance bond numbers, *n*, were generated for the M-O experimental bonded interactions comprising ten silicates, assumed to consist of charge neutral atoms. The resulting bond numbers serve to rank the experimental bond length in terms of the power law regression expression

$$R(M\text{-}O) = 1.39(n/r)^{-0.22} \qquad \text{Eq. (1)}$$

where r is the row number of the M atom (Boisen et al., 1988). This expression is comparable with an exponential expression used to rank the lengths of the C-C, C=C and C≡C bonded interactions within hydrocarbon molecules in terms of their resonance bond numbers and the number of electrons used in the bonded interactions.

A search for a nexus between the Pauling bond strength and the electron density between bonded pairs of atoms

With the perfection of the single crystal diffractometer, starting in the 1950's, together with the advent of the high speed computer and the coding of software for the recording of precise single crystal diffraction data for solving and refining crystal structures, it became apparent that connections exist between the bond lengths in a structure and the bond strengths and the bond strength sums, ζ, reaching the oxide anions for the associated bonded interactions. The world renowned mineralogist J.V. Smith (1953) was one of the first to discover that a connection exists between the ζ–values for the oxide anions in the mineral melilite and the lengths of the Si-O bonded interactions involving these anions. The experimental Si-O bond lengths, R(Si-O), in melilite were observed to increase progressively from 1.59 Å to 1.65 Å as the sum of the bond strengths, ζ, reaching the O atoms increases from 1.45 v.u. to 2.9 v.u. Shortly thereafter, Baur (1956) reported a similar correlation between ζ and bond lengths for a variety of different M-O bonded interactions, and established linear plots and expressions, based on Δζ values and individual mean bond lengths, that he used to reproduce the bond lengths for a number of bonded interactions for a variety of oxides. Zachariasen (1963; 1954) followed by Zachariasen and Plettinger (1959) found comparable trends between R(B^{3+}-O) and R(U^{6+}-O) bond lengths and bond strength sums. In a crystal chemical study of eight clinopyroxenes, Clark et al. (1969) showed that the R(B-O) values determined by Zachariasen (1963) decrease linearly with increasing bond strength, *s*, of the bonded interactions,

while the R(Si-O) values observed for pyroxenes were found to decrease quadratically with increasing *s*.

An empirical bond length, R(M-O), bond valence, s_o, power-law regression relationship,

$$R(M\text{-}O) = (s/s_o)^{-1/N} \quad \text{Eq. (2)}$$

was subsequently proposed by Brown and Shannon (1973), closely following the pioneering work of Donnay (1969) and Donnay and Allmann (1970). Starting with the experimental M-O bond lengths and bond strengths provided by the S&P (1969) tables, the parameters s_o and N were determined for more than 25 M-O individual bonded interactions where the ζ–value was constrained, by regression methods, in each case to match the valences of the cations., The sum of the resulting bond valences (bond strengths) for each of the M-O bonded interactions was found to match, on average within 5%, the formal values of the cations, attesting to the goodness of fit of the data.

Upon undertaking a molecular orbital theory interpretation of the second rule, the Pauling bond strengths for bonded interactions were found to be highly correlated with the Mulliken bond overlap populations, *n*(M-O), calculated for a number of geometry optimized M-O bonded interactions. The greater the bond strength, the greater the Mulliken population of the charge density associated with the bonded atoms, and the shorter the M-O bond lengths (Burdett and McLarnan, 1984; Gibbs, 1982). On the basis of this connection, Gibbs equated the Pauling bond strength with the bond number, and considered the Donnay and Allmann (1970) and Brown and Shannon (1973) bond length-bond valence curves to have the same meaning and significance as the well-known C-C bond length bond-number curves determined for hydrocarbon molecules (Pauling, 1960).

Following Pauling's (1960) assertion that his rules may be expected to hold for molecules, Gibbs et al. (1987) undertook a geometry optimization of the M-O bond lengths for more than 30 hydroxy

548 acid molecules. The averaged geometry optimized bond lengths, <R(M-O)>, were examined in
549 terms of the averaged Pauling bond strengths, <*s*>, of the bonded interactions divided by the row
550 numbers, r, of the M atoms (Gibbs et al., 1987). The bond lengths were found to scatter along a
551 single trend when plotted in terms of the normalized bond strength, <*s*>/r, defined by the power law
552 regression expression

553 $$<R(M\text{-}O)> = 1.39(<s>/r)^{-0.22} \qquad \text{Eq. (3)}$$

554 an expression that is identical in form with Eq. 1 that was found for the resonating bond number
555 strengths for the experimental M-O bonded interactions in silicate crystals. The correspondence
556 between *s* and *n* is consistent with Pauling's assertion that a rule equivalent to his electrostatic
557 valence rule but involving resonance bond numbers instead of bond strengths would express the
558 satisfaction of the valences for the nonmetal atoms for the silicates. Rewriting Eqs 1 and 3 in terms
559 of *n* and <s>, respectively, $n = r(1.39/R(M\text{-}O))^{4.54}$ and $<s> = r(1.39/R(M\text{-}O))^{4.54}$, we see that *n* and
560 <s> are numerically equal for a given bond length despite their different bases. If the ionic
561 electrostatic bond strength, *s*, of a bonded interaction is defined as the electrostatic charge of a
562 bonded cation divided by its coordination number, and if the resonance bond number strength, *n*, is
563 defined as the number of valence electrons of a charge neutral metal atom involved in a bonded
564 interaction, both divided by the coordination number, then *s* and *n* are exactly equal for a given bond
565 length. Pauling (1939) was well aware of the connection between bond strength and resonance bond
566 number when he wrote " If the bonds resonate among alternate positions, the valence of a metal
567 atom will tend to be divided equally among the bonds to the coordinating atoms, and a rule
568 equivalent to the electrostatic valence rule would express the satisfaction of the valences of the
569 nonmetal atoms.'

570 Extending the molecular orbital approach to the bonded interactions in crystals, Gibbs et al. (1987)
571 found that the average experimental M-O bond lengths and bond strengths provided by the S&P
572 (1969) tables for a large number of oxide crystals can be modeled with a comparable expression

573 $$<R(M\text{-}O)> = 1.43(<s>/r)^{-0.21} \qquad \text{Eq.(4)}$$

574 for the M atoms for six rows of the periodic table. The similarity between this equation and Eq. 3 is
575 compelling evidence that a close connection exists between bond lengths and bond strengths for both
576 molecules and crystals, a result that is consistent with Pauling's assertion that his rules for crystals
577 have significance for molecules. Further, in contrast with Eq. (2), which involves different sets of s_o
578 and N parameters for each of the individual M-O bonded interaction, Eqs (3) and (4) are global in
579 their application and hold for the bulk of M atoms in the periodic table when bonded to oxygen
580 atoms. Brown (1981) carefully derived more than 150 different sets of parameters, a pair of
581 parameters for each bonded pair, rather than a single parameter pair that would suffice globally for
582 all bonded interactions. Despite the restricted application of the model, Bickmore et al. (2013)
583 recently found that the model provides a fairly representative picture of the spatial distribution of the
584 bonded interactions about an atom. On the basis of this representation, Brown (2013) was quick to
585 point out that this advance may ultimately result in a basis for not only predicting bond angles but
586 ultimately predicting crystal structures.

587 As reported above, the power law relationships between <R(M-O> and <*s*>/r and *n*/r, respectively,
588 suggest that <*s*> is a direct measure of the average electron density between a pair of M-O bonded
589 interactions: the greater the value of <*s*>, the greater the value of *n*, the greater the value of $<\rho(\mathbf{r}_c)>$,
590 and the shorter the M-O bond lengths for both molecules and crystals alike. In a preliminary study of
591 this possibility, a regression analysis of the power law connection between <R(M-O)> and $<\rho(\mathbf{r}_c)>$

592 for a limited data set comprising an assortment of molecules and crystals (Gibbs et al., 2001),
593 resulted in the expression

594 $$<R(M\text{-}O)> = 1.47(<\rho(\mathbf{r}_c)>/r)^{-0.18} \qquad \text{Eq. (5)}$$

595 Although Eq. (5) is not identical to Eq. (4), it is similar in form. With the goal of establishing a more
596 accurate expression based on a more accurate and comprehensive set of values, $\rho(\mathbf{r}_c)$-values were
597 calculated for a large number of individual bonded interactions for three perovskite crystals,
598 $LaAlO_3$, $CaSnO_3$ and $YAlO_3$. The structures of these perovskites were geometry optimized within
599 the framework of density functional theory over a wide range of pressures: from ambient conditions
600 to 20 GPa for the first two perovskites, and up to 80 GPa for the third (Gibbs et al., 2012). A power
601 law regression analysis of the combined geometry optimized Al-O, Ca-O, Sn-O, Y-O and La-O bond
602 lengths and the $\rho(\mathbf{r}_c)/r$ values, resulted in the power law equation

603 $$R(M\text{-}O) = 1.41(\rho(\mathbf{r}_c)/r)^{-0.21} \qquad \text{Eq, (6)}$$

604 an expression that is strikingly similar in form to Eq. (3). The similarity between the two expressions
605 is further evidence for the existence of a one-to-one correspondence between the Pauling strength for
606 a bonded interaction and the electron density at the bond critical points for bonded pairs of atoms in
607 both molecules and crystals. Moreover, this correspondence applies for bonded interactions in
608 crystals at both high pressures and under ambient conditions. Rewriting Eq. 3 in terms of <s> and
609 Eq. 6 in terms of $\rho(\mathbf{r}_c)$, we find that $<s> = r(1.39/R(M\text{-}O))^{4.54}$ and $\rho(\mathbf{r}_c) = r(1.41/R(M\text{-}O))^{4.76}$, a result
610 that shows that <s> and $\rho(\mathbf{r}_c)$ display similar values, which typically agree to within ~ 5%, for a
611 given bond length and r value. The widespread use of the Brown-Shannon bond valence model in
612 mineralogy and material science owes much of its success to the direct connection that exists
613 between bond strength and the quantum mechanical observable, the electron density distribution.

As observed above, the values of the electron density, $\rho(\mathbf{r}_c)$, at r_c between the bonded pairs of M and O atoms and the associated bcp properties were calculated (Gibbs et al., 2001; Gibbs et al., 2008c; Kirfel et al., 2005) for a large number of bonded interactions measured for more than 55 oxide and silicate crystals containing non-transition and transition metal atoms from the first three rows of the periodic table. For each of the bonded interaction types, the experimental bond lengths were found to be highly correlated with $\rho(\mathbf{r}_c)$: the larger the accumulation of ED at $\mathbf{r}_c$, the greater the strength of the bonded interaction and, typically, the shorter the M-O bond length. To obtain representative estimates, consistent with the central limiting theorem of the value of the ED between the bonded atoms, the individual values of $\rho(\mathbf{r}_c)/r$ and the associated experimental bond lengths for each the bonded interactions were averaged in the same way that the experimental bond lengths were averaged by S&P (1969) when determining their effective ionic and crystal radii. The resulting averaged $<R(M\text{-}O)>$ and $<\rho(\mathbf{r}_c)/r>$ values, together with the individual R(M-O) and $\rho(\mathbf{r}_c)/r$ values determined for the perovskites studied, are plotted in Figure 4. A regression analysis for the combined data sets resulted in the same power law regression equation determined above for the perovskites (Gibbs et al., 2012)

$$<R(M\text{-}O)> = 1.41(<\rho(\mathbf{r}_c)>/r)^{-0.21} \qquad \text{Eq. (7)}$$

The data points in Figure 4 for bond lengths between 1.4 Å and 3.0 Å follow the trend defined by Eq. 7 for the M atoms from all five rows of the periodic table. However, for the shorter ^{IV}B-O, ^{III}B-O, ^{III}C-O and ^{III}N-O bond lengths that involve the more electronegative first row atoms and are more shared covalent in nature, the $<\rho(\mathbf{r}_c)>/r$ values fall systematically above the curve, revealing that their experimental bond lengths are systematically longer than the ones determined by Eq. 7.

The ED distributions for the bonded interactions used to prepare Figure 4 resemble the procrystal representations of the ED distributions, denoted $\rho(\mathbf{r}_c)^{pro}$, calculated for row 1 and 2 M atoms (Downs

et al., 2002). A procrystal distribution consists of the superposition of the ED distributions for non-interacting, neutral ground state atoms with spherically averaged ED distributions, clamped at the experimental positions that they occupy in the crystal (Gibbs et al., 1992). This connection was explored by Gibbs et al., (2013a) and the $\rho(\mathbf{r}_c)^{pro}/r$ values for the row 1-2 M-O bonded interactions, plotted as open bullets in terms of <R(M-O)> in Figure 4. As displayed in the figure, the $<\rho(\mathbf{r}_c)>^{pro}/r$ values follow the general trend defined by the $<\rho(\mathbf{r}_c)>/r$ and <R(M-O)> data sets, but as expected the $<\rho(\mathbf{r}_c)>/r$ values are significantly larger than the $<\rho(\mathbf{r}_c)>^{pro}/r$ values, particularly for the more shared covalent ^{III}N-O, ^{III}C-O and ^{III}B-O bonded interactions. For the more electropositive atoms, the two trends typically agree to within ~ 0.05 e/Å^3 with the $<\rho(\mathbf{r}_c)>^{pro}/r$ values tending to be less than the $<\rho(\mathbf{r}_c)>/r$ values for the Si-O, P-O and S-O bonded interactions. For the longer Ca-O, Sn-O, K-O, Y-O and La-O bonded interactions, $<\rho(\mathbf{r}_c)>/r \sim <\rho(\mathbf{r}_c)>^{pro}/r$. In cases where $<\rho(\mathbf{r}_c)>/r$ and $<\rho(\mathbf{r}_c)>^{pro}/r$ are in close agreement, as in the case of the Si-O bond, the ED between the bonded atoms is consistent with Pauling's (1948) claim that the atoms in crystals are largely devoid of charge, in effect being largely neutral and atomic. He pointed out, for example, that it has been customary to describe a cubic crystal like BaO as a checkerboard pattern of Ba^{2+} cations and O^{2-} anions bonded together by electrostatic bonded interactions. But, according to his *postulate of electrostatic neutrality*, a description of the structure as consisting of an arrangement of electrostatic bonded highly charged Ba^{2+} and O^{2-} ions would be a poorer description than one consisting of neutral Ba and O atoms, resulting in an ED distribution that would be classified as largely atomic. As this seems to be the case for the bonded interactions for oxides, then the electrostatic bond strength of a M-O bonded interaction serves as a direct measure of the resonance bond number as noted above. Accordingly, the greater the number of shared electrons in lieu of M cation charge, the

greater the value of the resonance number, the greater the bond strength, and the shorter the bond length (cf. Figure 4 in Brown and Shannon, 1973).

Given the nexus between resonance bond number and the number of shared electrons, the question that comes to mind is "How similar are the $<\rho(\mathbf{r}_c)>$ values defined by Eq. 7 and the Pauling empirical bond strengths, $s = z/\nu$, for M-O bonded interactions of given lengths in the coordination polyhedron in a crystal?" Recasting Eq. 7 in terms of $<\rho(\mathbf{r}_c)>$, we obtain

$$<\rho(\mathbf{r}_c)> = r(1.41/<R(M\text{-}O)>)^{4.76}. \qquad \text{Eq. (8)}$$

A calculation of $<\rho(\mathbf{r}_c)>$ for the average Si-O bonded length, $<R(Si\text{-}O)> = 1.623$ Å, observed for the tetrahedral SiO_4 oxyanions in silicates (Baur, 1981), results in $<\rho(\mathbf{r}_c)> = 1.02$ e/Å^3, which is comparable with the Pauling bond strength of 1.0 v.u. The average ^{VI}Si-O bond length, 1.774 Å, observed in stishovite results in a $<\rho(\mathbf{r}_c)>$ value of 0.67 e/Å^3, which concurs with $s = 0.67$ v.u. (Kirfel et al., 2001). The agreement between $<\rho(\mathbf{r}_c)>$ and s for these two Si-O bonded interactions may not be surprising, particularly given that the calculated bond lengths and $\rho(\mathbf{r}_c)$ values were used in the derivation of Eq. 8. The agreement in these two cases is satisfactory, but the agreement is much less satisfactory for bonded interactions involving the much more electronegative first row atoms ^{III}N, ^{III}C and ^{III}B where the values of $<\rho(\mathbf{r}_c)>$ are as much as 15 % larger than s.

In an examination of the extent to which the $<\rho(\mathbf{r}_c)>$ values generated with Eq. 8 agree with the individual s values for other bonded interactions, a set of reliable bond lengths is required. Convenient for this purposes is the set of reliable bond lengths that are obtained by simply adding Shannon's oxide anion crystal radius (1.24 Å) to the 'reliable radii' for the M cations given in Shannon's (1976) Table 1. For example, in the case of the $^{VIII}U^{+6}$- O bonded interaction, R($^{VIII}U^{+6}$-O) was estimated by adding 1.24 Å to 1.14 Å, where 1.14 Å is the reliable radius for the eight-coordinate U^{+4} cation i.e. $<R(^{VIII}U^{+4}\text{- O})> = 1.14$ Å + 1.24 Å = 2.38 Å. According to Eq. 8, $<\rho(\mathbf{r}_c)>$

682 $= 6(1.41/2.38)^{4.76} = 0.50$ e/Å^3 , which is comparable to the Pauling bond strength of $s = 0.50$ v.u. The
683 <s>-value calculated with the same bond length and Eq. 3 is 0.52, which is also in satisfactory
684 agreement with s. The agreement between $<\rho(\mathbf{r}_c)>$ and s is likewise satisfactory for the ^{IV}P-O
685 bonded interaction where $<R(^{IV}P\text{-}O)> = 1.55$ Å, $<\rho(\mathbf{r}_c)> = 1.27$ e/Å^3 and $s = 1.25$ v.u., and for ^{IV}S-
686 O where $<R(^{IV}S\text{-}O)> = 1.50$ Å, $<\rho(\mathbf{r}_c)> = 1.49$ e/Å^3 and $s = 1.50$ v.u.. These values and those
687 calculated with the reliable bond lengths generated with the remaining reliable radii in the Shannon
688 Table, are compared in Figure 5 in terms of the individual Pauling bond strengths, s, for the M-O
689 bonded interactions. Despite the relatively wide scatter of the resulting data set about the 45^o line, a
690 regression analysis of the data set reveals that more than ~ 95 % of the variation in $<\rho(\mathbf{r}_c)>$ can be
691 explained in terms of a linear dependence on the Pauling bond strength for the M-O bonded
692 interactions (Gibbs et al., 2013a). As implausible as it may seem, the regression line is statistically
693 identical with a one-to-one relationship between value of the ED at the bcp, $<\rho(\mathbf{r}_c)>$, and the classic
694 individual Pauling bond strengths for the M-O bonded interactions in molecules and crystals.
695 Furthermore, rewriting Eq. 4 in terms of s, $s = r(1.43/R(M\text{-}O))^{4.76}$, we see that $s \approx \rho(\mathbf{r}_c) =$
696 $r(1.41/R(M\text{-}O))^{4.76}$. This again demonstrates the remarkable relationship that exists between the
697 Pauling bond strength, the experimental bond lengths and the electron density distribution between
698 the bonded atoms. This is testament to Pauling's genius in choosing a simple parameter like bond
699 strength as a measure of the strength of a bonded interaction.

700 **Implications**

701 We have shown that the experimental and calculated ED distributions for siloxane molecules and
702 silicate crystals have yielded important information about the sizes of atoms along bond vectors,
703 results that show that the bonded radius of the O atom is strongly impacted by its bonded atoms. In
704 particular, the greater the electronegativity of the bonded atom, the greater the impact on the

distribution along the bond vectors. We also found that the bcp properties of these two groups are virtually indistinguishable, implying that the local bonded interactions for the molecules are virtually same as those observed for silicates. The accumulation of the electron density between bonded pairs of M-O bonded interactions, $\rho(\mathbf{r}_c) = r(1.41/R(M\text{-}O))^{4.76}$, correlates with the Pauling bond strengths of the individual bonded interactions on a one to one basis, implying that the bond strength is a direct measure of the accumulation of the ED between a bonded pair. The nexuses established between the bond lengths and <s>/r values for nitride, fluoride and sulfide molecules and crystals (Bartelmehs et al., 1989; Buterakos et al., 1992; Nicoll et al., 1994; Pyykko, 2012) implies that a nexus may also hold for $<\rho(r_c)>$.

Further, a comprehensive study of the bonded interactions undertaken for thioarsenides and arsenates, cases involving long-range Lewis acid-base directed van der Waals bonded interactions (Gibbs et al., 2009; Gibbs et al., 2011), indicates that the molecules are bonded into molecular crystals by bond paths of ED that link and align the Lewis base-acid regions in a key-lock fashion. As such, the bonded interactions between the molecules classifying as long range Lewis acid-base directed van der Waals intermolecular interactions. The ED distribution comprising the bond paths is asserted to be fundamental to the understanding of the self-assembly of the molecules in the formation of the crystals. A self assembly mechanism is proposed for the molecular crystals condensed from aqueous species that maximizes the number of Lewis acid-base bonded interactions, with the resulting directed bond paths structuralizing the molecules as molecular crystals (Gibbs et al., 2011). With *ab initio* quantum computational methods capable of describing both short-range intramolecular and long range London dispersion interactions arising from electron correlation, analyses of the dimers of As_4S_4 and As_4O_6 molecules cut from the structures of realgar and arsenolite, respectively, reveal that the molecules adopt a configuration that is virtually identical

with that observed in the crystals. Decomposition of the interaction energies, using symmetry adapted perturbation theory, reveals that both model dimers feature significant stabilization from electrostatics forces as anticipated by the Lewis acid/Lewis base picture of the interactions.

In an assessment of the role played by intermolecular forces in the self assembly of nanoparticle entities into large structures and materials, (Bishop et al., 2009) concluded that "The formation of most assemblies can be modeled and justified only *a posteriori,* and there are few examples in which the course of nanoscale self-assembly was predicted *a priori* from a knowledge of the individual interactions. In the study of the self-assembly of the arsenate and realgar molecules, a model was proposed based on directed, long ranged intermolecular interactions associated with the formation of Lewis acid-Lewis base complexes that not only serve as an *a priori* basis for understanding how molecules self-assemble in the formation of molecular crystals but also serves as a model for predicting the self assembly of nanoparticles in the formation of oxide and sulfide Lewis acid-base complexes.

The foregoing studies show promise of the things that will likely be rendered in the future about the properties of a material that are inherent in the ED distribution. As more and more such studies are undertaken and completed, our understanding of the properties and the bonded interactions is destined to enrich our understanding of the crystal chemistry of minerals. It is exciting to anticipate the new insights that will surely be forthcoming as the electron density distribution of minerals and related materials is explored in greater detail, such as the discovery of bond paths between the O atoms comprising the shared polyhedral edges of a crystal, the shorter the shared edges, the greater the values of $\rho(\mathbf{r}_c)$ and the greater the stabilization of the shared O-O edges as embodied in Pauling's third rule (Gibbs et al., 2008a).

Finally, the close connection between the bonded interactions in siloxane molecules and silicate crystals is consistent with the recent use of small molecular clusters in the study of mineral surfaces, studies that have provided new and important insights into the cleavage of bonded interactions, and the reactivity and hydrolytic reactions of surfaces at the atomic level (Casey and Rustad, 2007; Casey et al., 2009; Rosso, 2001; Rustad, 2001). Silica cluster calculations lend important insights into the hydrolysis of the Si-O-Si bonded linkages in the silica polymorph cristobalite (Pelmenschikov et al., 2001), the dissolution of silicate glass and mineral surfaces (Criscenti et al., 2006; Tamada et al., 2012) and providing evidence for the role played by aqua ions in the hydrolysis of Si-O bonded interactions (Wallace et al., 2010). The close connection established between the bonded interactions for sulfide crystals and molecules (Bartelmehs et al., 1989), also implies that the crystal-molecule nexus will be useful in the study of sulfide reactions. Indeed, recent advances in the development of theoretical tools to study sulfide surfaces, crystal growth, metal sulfide complexes, molecular clusters like oxides, have been used, not only to provided new insights into dissolution and surface reactions, but also to provide insights into crystal growth and the rapid self-assembly reactions at the atomic level that are involved in the formation of nanoparticles (cf. Rickard and Luther, 2006; Rosso and Vaughan, 2006a; Rosso and Vaughan, 2006b).

In short, the strikingly similarity in the structures and electron density distributions displayed by siloxane molecules and silicate crystals has provided an important basis for understanding the Si-O bonded interactions and the crystal chemistry of silicates at the atomic level. Likewise, the employment of small representative molecular clusters and related complexes has provided important insights into the reactions at mineral surfaces, the cleavage of bonded interactions at the atomic level, and crystal growth processes. The advances and insights provided by these studies together with their implications bring to mind the statement made by the brilliant crystal chemists

Michael O'Keeffe and Bruce Hyde (1981): 'The divorce of crystal chemistry (solid-state chemistry) from molecular chemistry was a great mistake and has left both parties all the poorer.'

Acknowledgements

This work was supported in part by the National Science Foundation and the U.S. Department of Energy through grants to N.L.R. (Grant Nos. MSF EAR-0738692 and EAR-1118691) and D.F.C. (Grant No. DE-FG02-97ER14751). K.M.R. acknowledges support from US Department of Energy (DOE), Office of Basic Energy Sciences, Chemical Sciences, Geosciences and Biosciences Division. G.V.G. is pleased to acknowledge Virginia Tech for its continued support over the last 15 years in his retirement. This contribution profited substantially from the insightful comments and valuable suggestions made by Professor Berry R. Bickmore at Brigham Young University, Professor Gordon E. Brown, Jr. at Stanford University and an unknown reviewer. The precious time that they spent carefully reading and evaluating the manuscript and pointing out a number of inconsistencies, defects and silly mistakes together with their important suggestions and valuable recommendations were greatly appreciated and resulted in a much improved copy. Professor Michael Hochella is thanked in particular for urging us to write the paper, a paper that would not have seen the light of day without his infectious encouragements and enthusiasm.

References

Ahrens, L.H. (1952) The use of ionization potentials Part 1. Ionic radii of the elements. Geochimica et Cosmochimica Acta, 2, 155-169.

Bader, R.F.W. (1990) Atoms in Molecules. Oxford Science Publications, Oxford, UK.

Bader, R.F.W. (2009) Bond paths are not chemical bonds. Journal of Physical Chemistry A, 113, 10391-10396.

797 Barlow, W. (1883) Probable nature of the internal symmetry of crystals. Nature, 29, 186-188.

798 Barlow, W. (1898) XXVI. Geometrische Untersuchung uber eine mechanische Ursache der
799 Homogenitat der Structur und der Symmetrie; mit besonderer Anwendung auf Krystallisation
800 und chemische Verbindung. Zeitschrift fur Kristallographie und Mineralogie, 29, 433-588.

801 Bartelmehs, K.L., Gibbs, G.V., and Boisen, M.B. (1989) Bond-length and bonded-radii variations in
802 sulfide molecules and crystals containing main-group elements; a comparison with oxides.
803 American Mineralogist, 74(5-6), 620-626.

804 Baur, W.H. (1956) über die Verfeinerung der Kristallstrukturbestimmung einiger Vertreter des
805 Rutiltyps: TiO_2, SnO_2, GeO_2 and MgF_2. Naturwissenschaften, 48, 549-552.

806 Baur, W.H. (1981) Interatomic Distance Predictions for Computer Simulation of Crystal Structures.
807 Structure and Bonding in Crystals, 2, 31-52. Academic Press, New York.

808 Bickmore, B.R., Wander, M.F.C., Edwards, J., Maurer, J., Shepherd, K., Meyer, E., Johansen, W.J.,
809 Frank, R.A., Andros, C., and Davis, M. (2013) Electronic structure effects in the vectorial
810 bond-valence model. American Mineralogist, 98, 340-349.

811 Bishop, K.J.M., Wilmer, C.E., Soh, S., and Grzybowski, B.A. (2009) Nanoscale forces and their
812 uses in self-assembly. Small, 5(14), 1600-1630.

813 Bohórquez, H.J., and Boyd, R.J. (2009) Is the size of an atom determined by its ionization energy?
814 Chemical Physics Letters, 480, 127-131.

815 Boisen, M.B., Gibbs, G.V., and Zhang, Z.G. (1988) Resonance bond numbers: A graph-theoretic
816 study of bond length variations in silicate crystals. Physics and Chemistry of Minerals, 15,
817 409-415.

818 Bragg, W.H., and Bragg, W.L. (1913) The structure of the diamond. Proceedings of the Royal
819 Society of London. Series A, 89, 277-291.

820 Bragg, W.L. (1913) The structure of some crystals as indicated by their diffraction of X-rays.
821 Proceedings of the Royal Society of London. Series A, 89, 248-277.

822 Bragg, W.L. (1914) The analysis of crystals by the X-ray spectrometer. Proceedings of the Royal
823 Society of London. Series A, 89(613), 468-489.

824 Bragg, W.L. (1920) The arrangement of atoms in crystals. London, Edinburgh, and Dublin Phil.
825 Mag. J. Sci., 40, 169-189.

826 Bragg, W.L. (1937) Atomic Structure of Minerals. Cornell University Press, Ithaca, N.Y.

827 Brown, I.D. (2013) A step closer to predicting the bonding geometry of crystals. American
828 Mineralogist, 98, 1093-1094.

Brown, I.D., and Shannon, R.D. (1973) Empirical bond-strength-bond-length curves for oxides. Acta Crystallographica Section A, 29, 266-282.

Burdett, J.K., and McLarnan, T.J. (1984) An orbital interpretation of Pauling's rules. American Mineralogist, 69, 601-621.

Buterakos, L.A., Gibbs, G.V., and Boisen, M.B. (1992) Bond length variation in hydronitride molecules and nitride crystals. Physics and Chemistry of Minerals, 19, 127-132.

Cahen, D. (1988) Atomic radii in ternary adamantines. Journal of Physics and Chemistry of Solids, 49, 103-111.

Casey, W.H., and Rustad, J.R. (2007) Reaction dynamics, molecular clusters, and aqueous geochemistry. Annual Review of Earth and Planetary Sciences, 35, 21-46.

Casey, W.H., Rustad, J.R., and Spiccia, L. (2009) Minerals as molecules—Use of aqueous oxide and hydroxide clusters to understand geochemical reactions. Chemistry – A European Journal, 15, 4496-4515.

Clark, J.R., Appleman, D.E., and Papike, J.J. (1969) Crystal-Chemical Characterization of Clinopyroxenes Based on Eight New Refinements. In J.J. Papike, Ed. MSA Special Paper no. 2, p. 31-50.

Coulson, C.A. (1955) The Contributions of Wave Mechanics to Chemistry. Journal of the Chemical Society, 2069-2084.

Cremer, D., and Kraka, E. (1984) A Description of the Chemical Bond in Terms of Local Properties of Electron Density and Energy. Croat. Chem. Acta, 57(6), 1259-1281.

Criscenti, L.J., Kubicki, J.D., and Brantley, S.L. (2006) Silicate glass and mineral dissolution: Calculated reaction paths and activation energies for hydrolysis of a Q(3) Si by H_3O^+ using ab initio methods. Journal of Physical Chemistry A, 110(1), 198-206.

Donnay, G. (1969) Further Use for the Pauling-Bond Concept. Canegie Institute of Washington Yearbook, 68, 292-295.

Donnay, G., and Allmann, R. (1970) How to recognize O^{2-}, OH^-, and H_2O in crystal structures determined by X-ray. American Mineralogist, 55, 1003-1015.

Downs, R.T., Andalman, A., and Hudacsko, M. (1996) The coordination numbers of Na and K atoms in low albite and microcline as determined from a procrystal electron-density distribution. American Mineralogist, 81, 1344-1349.

Downs, R.T., Gibbs, G.V., Boisen Jr, M.B., and Rosso, K.M. (2002) A comparison of procrystal and ab initio model representations of the electron-density distributions of minerals. Physics and Chemistry of Minerals, 29, 369-385.

Fajans, K. (1931) Radioelements and Isotopes, Chemical Forces. Cornell University Press, Itaca, NY.

Feynman, R.P. (1939) Forces in molecules. Physical Review, 56, 340.

Friedrich, W., Knipping, P., and von Laue, M. (1912) Sitzungsberiche der mathematisch-physikalischen Klasse der Königlich. Bev. Bayer, Akad. Wiss. zu München, 302-322.

Fyfe, W.S. (1954) The Problem of Bond Type. American Mineralogist, 39, 991-1004.

Gatti, C. (1997) TOPOND96 User's Manual. CNR-CSRSRC, Milano, Italy.

Gatti, C. (2005) Chemical bonding in crystals: new directions. Zeitschrift Fur Kristallographie, 220, 399-457.

Gibbs, G.V. (1982) Molecules as models for bonding in silicates. American Mineralogist, 67, 421-450.

Gibbs, G.V., Boisen, M.B., Beverly, L.L., and Rosso, K.M. (2001) A computational quantum chemical study of the bonded interactions in earth materials and structurally and chemically related molecules. In R.T. Cygan, and J.D. Kubicki, Eds. Molecular Modeling Theory: Applications in the Geosciences, 42, p. 345-381. Mineralogical Society of America, Washington, DC.

Gibbs, G.V., Cox, D.F., and Rosso, K.M. (2004) A connection between empirical bond strength and the localization of the electron density at the bond critical points of the Si-O bonds in silicates. Journal of Physical Chemistry A, 108, 7643-7645.

Gibbs, G.V., Downs, R.T., Cox, D.F., Ross, N.L., Boisen, M.B., and Rosso, K.M. (2008a) Shared and closed-shell O-O interactions in silicates. Journal of Physical Chemistry A, 112, 3693-3699.

Gibbs, G.V., Downs, R.T., Cox, D.F., Ross, N.L., Prewitt, C.T., Rosso, K.M., Lippmann, T., and Kirfel, A. (2008b) Bonded interactions and the crystal chemistry of minerals: A review. Zeitschrift fur Krisstallographie, 223, 1-40.

Gibbs, G.V., Downs, R.T., Cox, D.F., Rosso, K.M., Ross, N.L., Kirfel, A., Lippmann, T., Morgenroth, W., and Crawford, T.D. (2008c) Experimental bond critical point and local energy density properties determined for Mn-O, Fe-O, and Co-O bonded interactions for tephroite, Mn_2SiO_4, fayalite, Fe_2SiO_4, and Co_2SiO_4 olivine and selected organic metal complexes: Comparison with properties calculated for non-transition and transition metal M-O bonded interactions for silicates and oxides. Journal of Physical Chemistry A, 112, 8811-8823.

Gibbs, G.V., Finger, L.W., and Boisen, M.B. (1987) Molecular mimicry of the bond length-bond strength variations in oxide crystals. Physics and Chemistry of Minerals, 14, 327-331.

Gibbs, G.V., Ross, N.L., Cox, D.F., Rosso, K.M., Iversen, B.B., and Spackman, M.A. (2013a) Bonded radii and the contraction of the electron density of the oxygen atom by bonded interactions. The Journal of Physical Chemistry A, 117, 1632-1640.

Gibbs, G.V., Ross, N.L., Cox, D.F., Rosso, K.M., Iversen, B.B., and Spackman, M.A. (2013b) Pauling bond strength, bond length and electron density distribution. Physics and Chemistry of Minerals, 1-9.

Gibbs, G.V., Spackman, M.A., and Boisen, M.B. (1992) Bonded and promolecule radii for molecules and crystals. American Mineralogist, 77(7-8), 741-750.

Gibbs, G.V., Wallace, A.F., Cox, D.F., Dove, P.M., Downs, R.T., Ross, N.L., and Rosso, K.M. (2009) Role of directed van der Waals bonded interactions in the determination of the structures of molecular arsenate solids. Journal of Physical Chemistry A, 113, 736-749.

Gibbs, G.V., Wallace, A.F., Downs, R.T., Ross, N.L., Cox, D.F., and Rosso, K.M. (2011) Thioarsenides: a case for long-range Lewis acid-base-directed van der Waals interactions. Physics and Chemistry of Minerals, 38, 267-291.

Gibbs, G.V., Wang, D., Hin, C., Ross, N.L., Cox, D.F., Crawford, T.D., Spackman, M.A., and Angel, R.J. (2012) Properties of atoms under pressure: Bonded interactions of the atoms in three perovskites. The Journal of Chemical Physics, 137, 164313.

Gibbs, G.V., Whitten, A.E., Spackman, M.A., Stimpfl, M., Downs, R.T., and Carducci, M.D. (2003) An exploration of theoretical and experimental electron density distributions and Si O bonded interactions for the silica polymorph coesite. Journal of Physical Chemistry B, 107, 12996-13006.

Goldschmidt, V.M. (1954) Geochemistry. 736 p. Clarendon Press, Oxford.

Hoffmann, R. (1988) Solids and Surfaces: A Chemist's View of Bonding in Extended Structures. 142 p. VCH Publishers, Inc, New York, NY

Hüttig, G.F. (1920) Notiz zur geometrie der koordinationzahl. Zeitschrift fur Anorganische und Allgemeine Chemie, 113, 24-26.

Johnson, O. (1973) Ionic radii for spherical potential ions. I. Inorganic Chemistry, 12, 780-785.

Johnson, W.R., Kolb, D., and Huang, K.N. (1983) Electric dipole, quadrupole, and magnetic-dipole susceptibilities and shielding factors for closed-shell ions of the He, Ne, Ar, Ni (Cu+), Kr, Pb, and Xe isoelectronic sequences. Atomic Data and Nuclear Data Tables, 28, 333-340.

Kirfel, A., Krane, H.G., Blaha, P., Schwarz, K., and Lippmann, T. (2001) Electron-density distribution in stishovite, SiO_2: a new high-energy synchrotron-radiation study. Acta Crystallographica Section A, 57, 663-677.

Kirfel, A., Lippmann, T., Blaha, P., Schwarz, K., Cox, D.F., Rosso, K.M., and Gibbs, G.V. (2005) Electron density distribution and bond critical point properties for forsterite, Mg_2SiO_4,

931 determined with synchrotron single crystal X-ray diffraction data. Physics and Chemistry
932 Minerals, 32, 301-313.

933 Muller, O., and Roy, R.R. (1974) The Major Ternary Structure Families. Springer-Verlag, New
934 York.

935 Nicoll, J.S., Gibbs, G.V., Boisen, M.B., Downs, R.T., and Bartelmehs, K.L. (1994) Bond length and
936 radii variations in fluoride and oxide molecules and crystals. Physics and Chemistry of
937 Minerals, 20, 617-624.

938 Novak, G.A., and Gibbs, G.V. (1971) The Crystal Chemistry of the Silicate Garnets. American
939 Mineralogist, 56, 791-825.

940 O'Keeffe, M., and Hyde, B.G. (1981) The role of nonbonded forces in crystals. In M. O'Keeffe, and
941 A. Navrotsky, Eds. Structure and Bonding in Crystals, 1, p. 222-254. Academic Press, New
942 York.

943 Parr, R.G., and Yang, W. (1989) Density-functional theory of atoms and molecules. 333 p. Oxford
944 University Press, Oxford.

945 Pauling, L. (1927) The sizes of ions and the structure of ionic crystals. Journal of the American
946 Chemical Society, 49, 765-790.

947 Pauling, L. (1929) The Principles Determining the Crystal Structure of Complex Ionic Crystals.
948 Journal of the American Chemical Society, 51, 1010-1026.

949 Pauling, L. (1939) The Nature of the Chemical Bond. Cornell University Press, Ithaca, NY.

950 Pauling, L. (1948) The modern theory of valency. Journal of the Chemical Society (Resumed), 0,
951 1461-1467.

952 Pauling, L. (1960) The Nature of the Chemical Bond and the Structure of Molecules and Crystals:
953 An Introduction to Modern Structural Chemistry. Cornell University Press, Ithaca, N.Y.

954 Pelmenschikov, A., Leszczynski, J., and Pettersson, L.G.M. (2001) Mechanism of dissolution of
955 neutral silica surfaces: Including effect of self-healing. Journal of Physical Chemistry A,
956 105(41), 9528-9532.

957 Pyykko, P. (2012) Refitted tetrahedral covalent radii for solids. Physical Review B, 85(2).

958 Rickard, D., and Luther, G.W. (2006) Metal Sulfide Complexes and Clusters. In D.J. Vaughan, Ed.
959 Sulfid Mineralogy and Geochemistry, 61, p. 421-504. Geochemical Society and
960 Mineralogical Society of America, Washington, D.C.

961 Rosso, K.M. (2001) Structure and Reactivity of Semiconducting Mineral Surfaces: Convergence of
962 Molecualr Modeling and Experiment. In R.T. Cygan, and J.D. Kubicki, Eds. Molecular
963 Modeling Theory: Applications in the Geosciences, 42, p. 199-271. Goechemical Society and
964 Mineralogical Society of Americs, Washington, D.C.

965 Rosso, K.M., and Vaughan, D.J. (2006a) Reactivity of Sulfide Mineral Surfaces. Reviews in
966 Mineralogy and Geochemistry, 61(1), 557-607.

967 -. (2006b) Sulfide Mineral Surfaces. Reviews in Mineralogy and Geochemistry, 61(1), 505-556.

968 Rustad, J.R. (2001) Molecular Models of Surface Relaxation, Hydroxylation, and Surface Charging
969 at Oxide-Water Interfaces. In R.T. Cygan, and J.D. Kubicki, Eds. Molecuar Modeling
970 Theory: Applications in the Geosciences, 42, p. 169-197. Geochemical Society and
971 Mineralogical Society of America, Washington, D.C.

972 Saunders, V.R., Dovesi, R., Roetti, C., Causa, M., Harrison, N.M., Orlando, R., and Apra, E. (1998)
973 CRYSTAL98 User's Manual. University of Torino, Torino, Italy.

974 Shannon, R.D. (1976) Revised effective ionic radii and systematic studies of interatomic distances in
975 halides and chalcogenides. Acta Crystallographica, Section A: Crystal Physics, Diffraction,
976 Theoretical and General Crystallography, 32(5), 751-67.

977 -. (1981) Bond distances in sulfides and a preliminary table of sulfide crystal radii. In M. O'Keeffe,
978 and A. Navrotsky, Eds. Structure and bonding in crystals, 2, p. 53-70. Academic Press, New
979 York, NY.

980 Shannon, R.D., and Fischer, R.X. (2006) Empirical electronic polarizabilities in oxides, hydroxides,
981 oxyfluorides, and oxychlorides. Physical Review B, 73(23).

982 Shannon, R.D., and Prewitt, C.T. (1969) Effective Ionic Radii in Oxides and Fluorides. Acta Cryst.,
983 B25, 925-946.

984 Sherman, J. (1932) Crystal Energies of Ionic Compounds and Thermochemical Applications. Chem.
985 Rev., 11(1), 93-170.

986 Slater, J.C. (1964) Atomic radii in crystals. Journal of Chemical Physics, 41(10), 3199-3204.

987 -. (1965) Quantum Theory of Molecules and Solids: Symmetry and Energy Bands in Crystals.
988 McGraw Hill, Inc., New York, NY.

989 Smith, J.V. (1953) Reexamination of the crystal structure of melilite. American Mineralogist, 38,
990 643-661.

991 Tamada, O., Gibbs, G.V., Boisen, M.B., and Rimstidt, J.D. (2012) Silica dissolution catalyzed by
992 NaOH: Reaction kinetics and energy barriers simulated by quantum mechanical strategies.
993 Journal of Mineralogical and Petrological Sciences, 107(2), 87-98.

994 Tosi, M.P. (1964) Cohesion of Ionic Solids in the Born Model. In S. Frederick, and T. David, Eds.
995 Solid State Physics, Volume 16, p. 1-120. Academic Press.

996 Tosi, M.P., and Fumi, F.G. (1964) Ionic sizes and born repulsive parameters in the NaCl-type alkali
997 halides—I I: The generalized Huggins-Mayer form. Journal of Physics and Chemistry of
998 Solids, 25(1), 45-52.

Wallace, A.F., Gibbs, G.V., and Dove, P.M. (2010) Influence of Ion-Associated Water on the Hydrolysis of Si-O Bonded Interactions. Journal of Physical Chemistry A, 114(7), 2534-2542.

Warren, B., and Bragg, W.L. (1928) The structure of diopside, $CaMg(SiO_3)_2$. Zeitschrift fur Kristallographie, 69, 168-93.

Warren, B.E. (1929) The structure of tremolite. Zeitschrift fur Kristallographie, 72, 42-57.

Wasasjerna, J.A. (1923) Radii of Ions. Soc. Sci. Fenn. Comm. Phys. Math., 38, 1-25.

Zachariasen, W. (1963) The crystal structure of monoclinic metaboric acid. Acta Crystallographica, 16(5), 385-389.

Zachariasen, W.H. (1954) Crystal Chemical Studies of the 5f-Series of Elements. XXIII. On the Crystal Chemistry of Uranyl Compounds and of Related Compounds of Transuranic Elements. Acta Crystallographica, 7, 795-799.

Zachariasen, W.H., and Plettinger, H.A. (1959) Crystal Chemical Studies of the 5f-Series of Elements. XXV. The Crystal Structure of Sodium Uranyl Acetate. Acta Crystallographica, 12, 526-530.

Zhang, Y.X., and Cherniak, D.J. (2010) Diffusion in Minerals and Melts Introduction. In Y.X. Zhang, and D.J. Cherniak, Eds. Diffusion in Minerals and Melts, 72, p. 1-4. Mineralogical Soc Amer, Chantilly.

1020

1021 **Table 1.** Comparison of Bonded, r_b, Crystal,r_c, and Ionic Radii, r_i.

^{CN}M	<r_b(M)>	r_c(M)	r_i(M)	<r_b(O)>	^{CN}M	<r_b(M)>	r_c(M)	r_i(M)	<r_b(O)>
^{IV}Al	0.74	0.53	0.39	1.00	^{VI}K	1.44	1.52	1.38	1.43
^{V}Al	0.78	0.62	0.48	1.08	^{I}H	0.19	-0.24	-0.38	0.79
^{VI}Al	0.80	0.68	0.54	1.12	^{VI}Li	0.82	0.90	0.76	1.39
^{III}As^{3+}	0.87			0.92	^{IV}Mg	0.84	0.71	0.57	1.07
^{III}B	0.46	0.15	0.10	0.91	^{V}Mg	0.90	0.80	0.66	1.17
^{IV}B	0.49	0.25	0.11	0.99	^{VI}Mg	0.94	0.86	0.72	1.20
^{IV}Be	0.58	0.41	0.27	1.07	^{VIII}Mg	0.96	1.03	0.89	1.31
^{III}C	0.46	0.06	-0.08	0.83	^{VI}Mn^{2+}	1.10	0.97	0.83	1.12
^{VI}Ca	1.18	1.14	1.00	1.18	^{VIII}Mn^{2+}	1.15	1.10	0.96	1.18
^{VII}Ca	1.22	1.20	1.06	1.23	^{III}N	0.60	0.04	-0.10	0.64
^{VIII}Ca	1.25	1.26	1.12	1.27	^{V}Na	1.08	1.14	1.00	1.36
^{IX}Ca	1.25	1.32	1.18	1.26	^{VI}Na	1.09	1.16	1.02	1.35
^{VI}Co^{2+}	1.05	0.72	0.58	1.08	^{VII}Na	1.12	1.26	1.12	1.40
^{IV}Fe^{2+}	0.98	0.77	0.63	0.99	^{IV}P	0.63	0.31	0.17	0.91
^{VI}Fe^{2+}	1.08	0.92	0.78	1.10	^{IV}S	0.58	0.26	0.12	0.89
^{VIII}Fe^{2+}	1.13	1.06	0.92	1.17	^{IV}Si	0.67	0.40	0.26	0.95
^{IV}Ge	0.83	0.53	0.39	0.91	^{VI}Si	0.72	0.54	0.40	1.06

1022

1023

FIGURE LEGENDS

Figure 1: Scatter diagrams of the experimental Si-O bond lengths, R(Si-O) Å, for a large number of silicate and oxide crystal structures plotted as open diamonds in terms (a) the accumulation of the electron density, ED, calculated at the bond critical point, $\mathbf{r}_c$, (b) $\lambda_{1,2}$, the magnitude of the average concentration of the ED calculated perpendicular to $\mathbf{r}_c$, (c) λ_3, the concentration of the ED at $\mathbf{r}_c$ calculated along bond path toward Si and O, (d) $\nabla^2\rho(\mathbf{r}_c)$, the Laplacian of the ED calculated at $\mathbf{r}_c$ and (f) the bonded radius of the O atom, r_b(O) bonded to Si. Superimposed on the figure are the bond critical properties for the Si-O bonded interactions observed for coesite and stishovite, plotted as solid triangles and squares, respectively (reproduced from Gibbs et al., 2004).

Figure 2: Experimental M-O bond lengths, R(M-O) Å, plotted in terms of the bond radii, r_b(O), of the O atoms bonded to first row (Li, Be, B,···) and second row (Na, Mg, Al,···) atoms for the silicate and oxide structures (reproduced from Gibbs et al., 2001).

Figure 3: Averaged experimental M-O bond lengths, <R(M-O)> Å, plotted in terms of the averaged bonded radii, r_b(M), for the M atoms bonded to O for first, second and third row M atoms.

Figure 4: Averaged experimental M-O bond lengths, <R(M-O)> Å, plotted in terms of the averaged value of electron density, $<\rho(\mathbf{r}_c)>/r$, accumulated at the bond critical point, $\mathbf{r}_c$, between bonded pairs of M and O atoms for M atoms for five row of the periodic table. The open circle data are procrystal data calculated for first and second row bonded interactions (Downs et al., 2002). The regression

equation, $<R(M\text{-}O)> = 1.41(<\rho(\mathbf{r}_c)>/r)^{-0.21}$, fit to all of the data with the exception of the procrystal data, is graphed as a solid curve on the figure. (Reproduced from Gibbs et al., 2013b)

Figure 5: Equation 7, $<\rho(\mathbf{r}_c)> = (1.41/<R(M\text{-}O)>)^{4.76}$, plotted in terms of the average Pauling strength, s, for the M-O bonded interactions comprising M-atom containing coordination polyhedron where the bond lengths $<R(M\text{-}O)>$ were set equal to the sum of Shannon's (1976) most reliable crystal radius for a given M cation and the radius of the four-coordinated oxide anion, 1.24 Å.

This is a preprint, the final version is subject to change, of the American Mineralogist (MSA)
Cite as Authors (Year) Title. American Mineralogist, in press.
(DOI will not work until issue is live.) DOI: http://dx.doi.org/10.2138/am.2014.4660

Figure 1

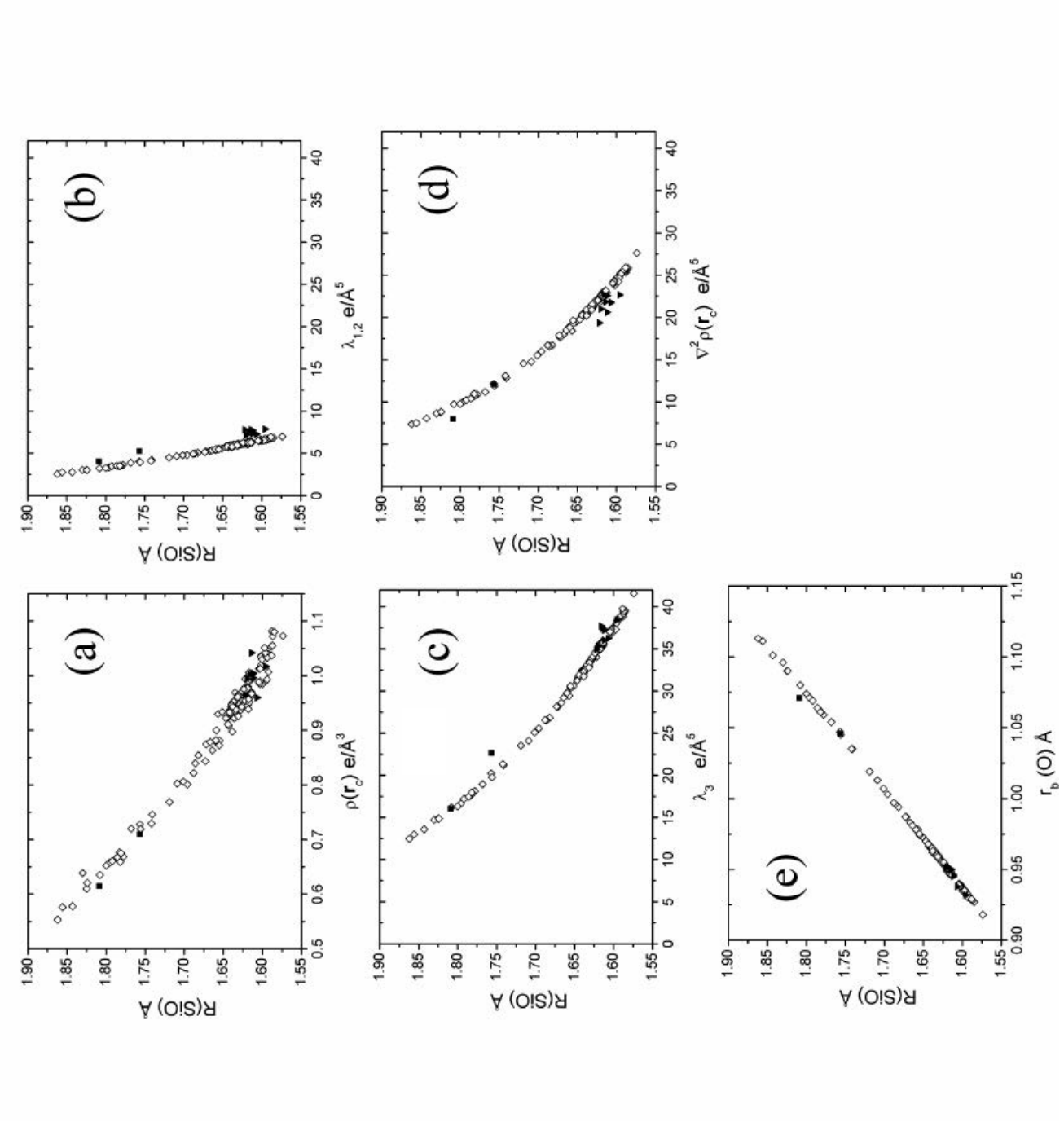

This is a preprint, the final version is subject to change, of the American Mineralogist (MSA)
Cite as Authors (Year) Title. American Mineralogist, in press.
(DOI will not work until issue is live.) DOI: http://dx.doi.org/10.2138/am.2014.4660

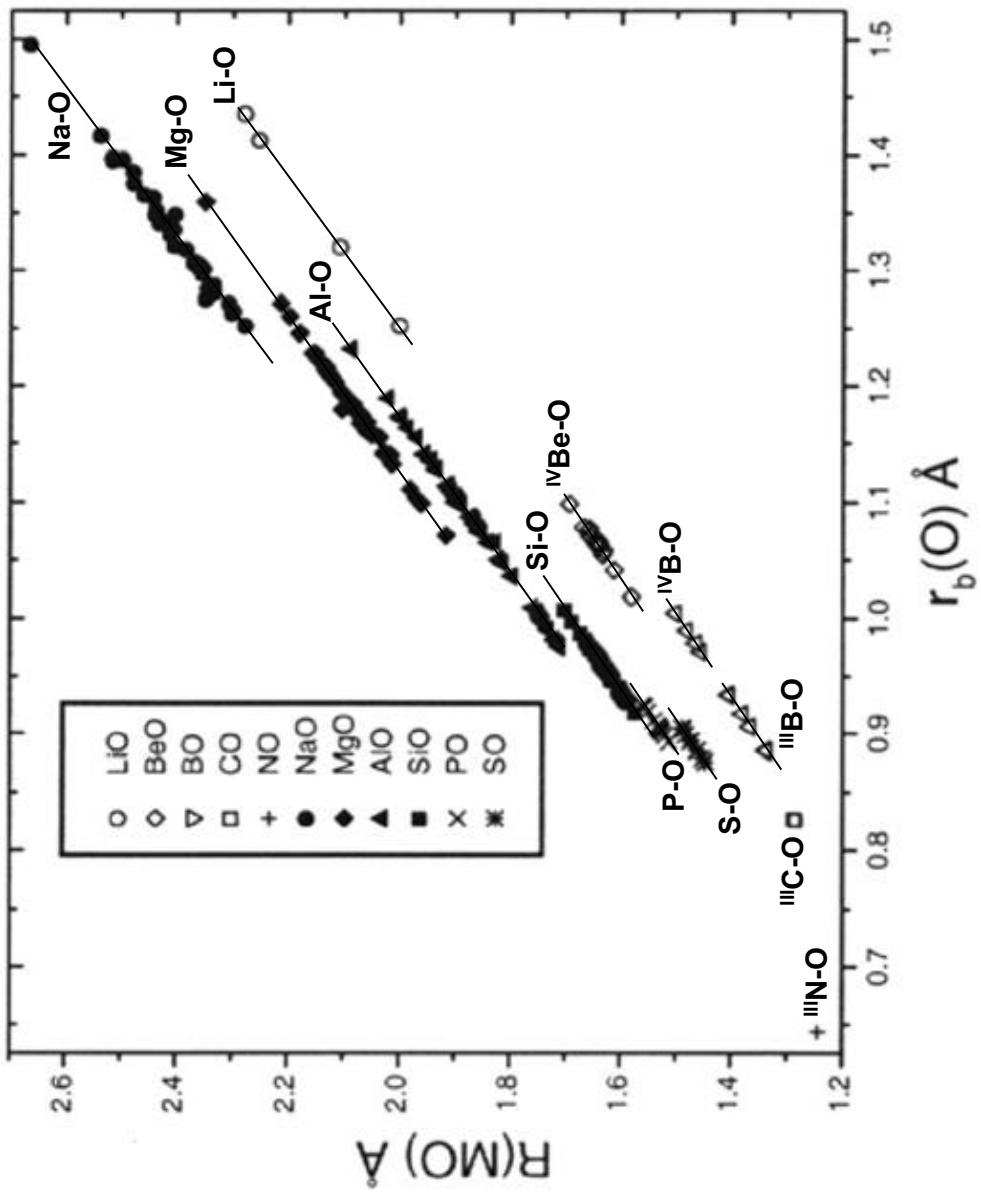

Figure 2

This is a preprint, the final version is subject to change, of the American Mineralogist (MSA)
Cite as Authors (Year) Title. American Mineralogist, in press.
(DOI will not work until issue is live.) DOI: http://dx.doi.org/10.2138/am.2014.4660

Figure 3

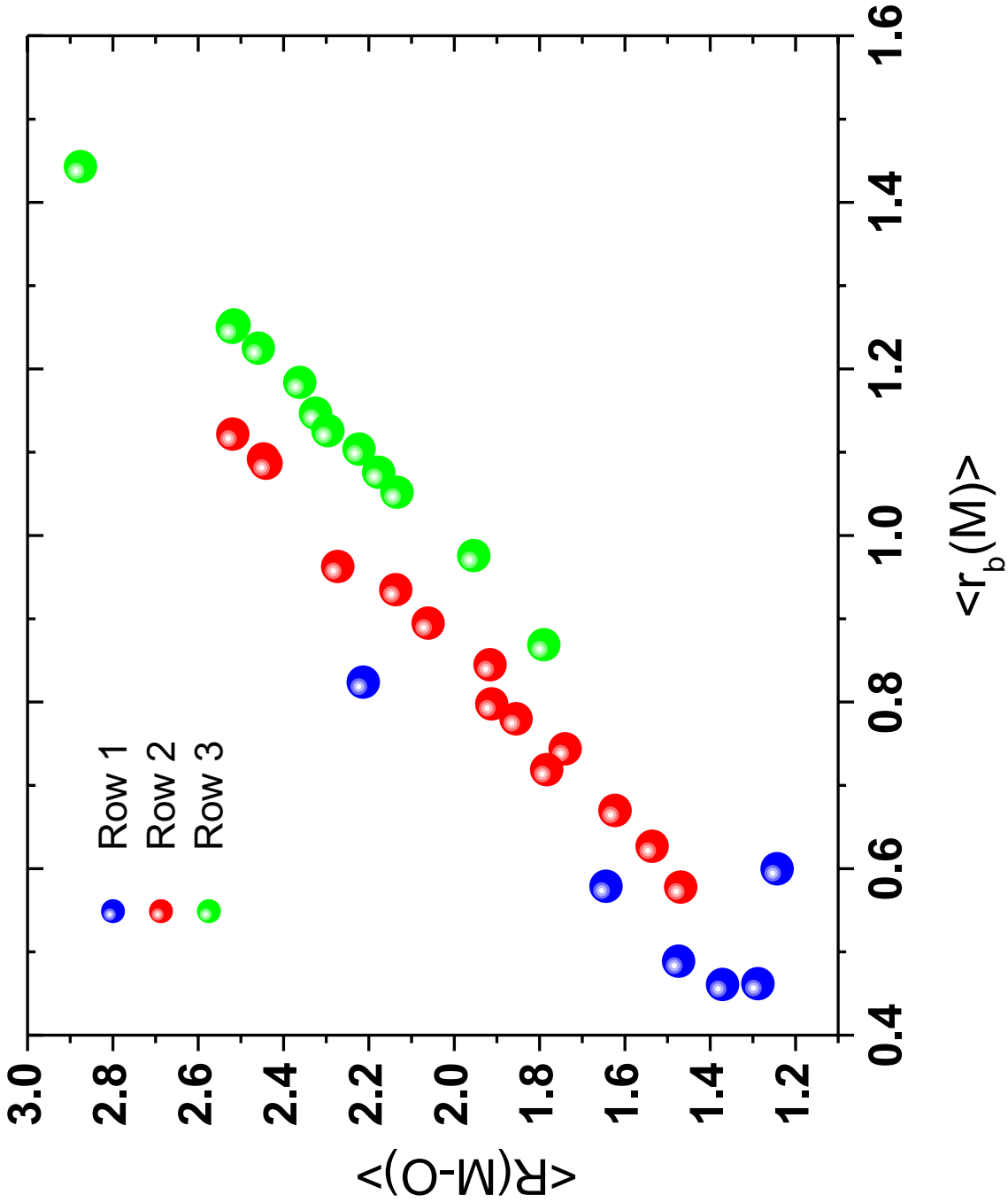

This is a preprint, the final version is subject to change, of the American Mineralogist (MSA)
Cite as Authors (Year) Title. American Mineralogist, in press.
(DOI will not work until issue is live.) DOI: http://dx.doi.org/10.2138/am.2014.4660

Figure 4

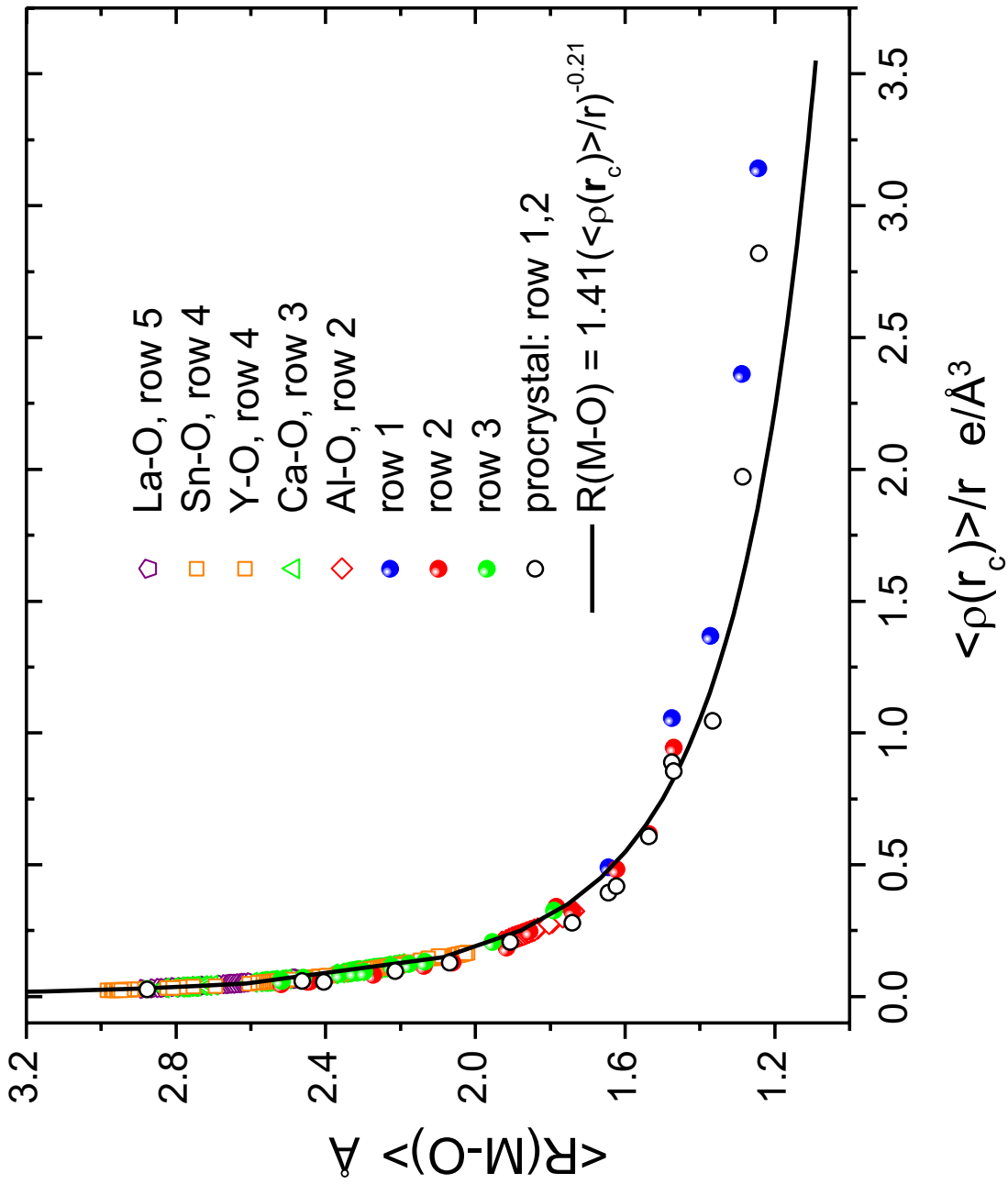

This is a preprint, the final version is subject to change, of the American Mineralogist (MSA)
Cite as Authors (Year) Title. American Mineralogist, in press.
(DOI will not work until issue is live.) DOI: http://dx.doi.org/10.2138/am.2014.4660

Figure 5